

PRODUCTION OF BIO-OIL FROM HAZELNUT SHELL WASTE BY USING SUPERCRITICAL ETHANOL, ACETONE AND THEIR MIXTURES

**A Thesis Submitted to
the Graduate School of Engineering and Sciences of
İzmir Institute of Technology
in Partial Fulfillment of the Requirements for the Degree of
MASTER OF SCIENCE
in Chemical Engineering**

**by
Orkan DAL**

**December 2018
İZMİR**

We approve the thesis of **Orkan DAL**

Examining Committee Members:

Assoc. Prof. Dr. Ash YÜKSEL ÖZŞEN

Department of Chemical Engineering, İzmir Institute of Technology

Asst. Prof. Dr. Ali Can KIZILKAYA

Department of Chemical Engineering, İzmir Institute of Technology

Prof. Dr. Levent BALLİCE

Department of Chemical Engineering, Ege University

26 December 2018

Assoc. Prof. Dr. Ash YÜKSEL ÖZŞEN

Supervisor, Department of Chemical
Engineering, İzmir Institute of Technology

Prof. Dr. Erol ŞEKER

Head of the Department of Chemical
Engineering

Prof. Dr. Aysun SOFUOĞLU

Dean of the Graduate School of
Engineering and Sciences

ACKNOWLEDGMENTS

Firstly, I would like to thank my advisor Assoc. Prof. Dr Aslı YÜKSEL ÖZŞEN for her support, encouragement and guidance during my M.Sc. thesis. I gained a lot of significant experiences in the study with the help of her research team. These experiences will carry with me my remaining life.

I am grateful to my teammate Emre DEMİRKAYA for his support, friendship throughout my experiments and analysis. In addition, I thank to research centre experts Handan GAYGISIZ for GC-MS analysis and Yekta GÜNAY OĞUZ for FT-IR analysis.

I would also like to thank my friends Emre DEĞİRMENÇİ, Bertan ÖZDOĞRU, Farid MUSA, Mete TOKGÖZ, Ozan CEYLAN for their support and helpful advice during the thesis period.

Finally, I would like to special thanks to my parents Nilüfer DAL and Efgan DAL, and my girlfriend Hazal AKSOY for their support and encouragements. This thesis could not be finished without them.

ABSTRACT

PRODUCTION OF BIO-OIL FROM HAZELNUT SHELL WASTE BY USING SUPERCRITICAL ETHANOL, ACETONE AND THEIR MIXTURES

The goal of this study was to investigate effect of reaction temperature, reaction time and solvent ratio (ethanol/acetone v/v%) on bio-oil yield, solid conversion and product distribution. Direct thermochemical biomass degradation to obtain bio-oil by using organic solvents is not a new process type, and it has some advantages over hydrothermal liquefaction technique. However, in literature, to our best knowledge, there is no study about hazelnut shell decomposition by using ethanol, acetone and their mixtures at sub/supercritical conditions. In this study, experiments were carried out between 220-300 °C, at three different temperatures (30, 60 & 90 min) for five different solvent ratios. Highest solid conversion achieved at 300 °C by using pure ethanol was 64.2%, whereas highest bio-oil yield was found as 44.2% at 300 °C with 50/50 (EtOH/Ac: v/v). Ethanol and acetone showed different characteristics during the experiments and their effect on the conversion and bio-oil yield were discussed. Statistical analysis showed that time, temperature, ratio and temperature-time are affecting parameters for the conversion and bio oil yield while time-ratio and temperature-ratio are not. According to GC-MS results, product distribution changed with respect to solvent type and ratio.

ÖZET

FINDIK KABUĞU ATIKLARINDAN KRİTİKÜSTÜ ETANOL, ASETON VE BU ÇÖZGENLERİN KARIŞIMLARI KULLANILARAK BİYO-YAĞ ELDESİ

Bu çalışmanın amacı, fındık kabuğu atıklarından kritiküstü etanol, aseton ve bu çözgenlerin karışımıları kullanılarak üretilen biyo-yağın veriminin, fındık kabuğu dönüşüm oranının ve ürün dağılımının, reaksiyon sıcaklığı, reaksiyon süresi ve çözgen oranlarından nasıl etkileneceğini araştırmaktır. Daha önce, fındık kabuğu atıkları kullanılarak kritiküstü etanol, aseton ve bu çözgenlerin karışımıları kullanılarak biyo-yağ eldesi literatürde araştırılmamıştır. Deneyler, sıcaklık olarak 220, 260 ve 300 °C, reaksiyon süresi olarak 30, 60, 90 dakika, 5 farklı etanol/aseton oranında yapılmıştır. En yüksek katı dönüşümü, saf etanol kullanılarak 300 °C'de 64.2% olarak elde edilirken; en yüksek biyo-yağ verimi, etanol/aseton hacimsel oranının 50/50% ve reaksiyon sıcaklığının 300 °C olduğu koşullarda 44.2% olarak bulunmuştur. Etanol ve aseton biyo-yağ veriminde ve katı dönüşümünde farklı etkilere sahiptir. İstatistiksel analiz sonucunda; reaksiyon sıcaklığı, reaksiyon süresi, çözgen oranları katı dönüşümü ve biyo-yağ verimi üzerinde etkiye sahipken, reaksiyon süresi*çözgen oranı ve reaksiyon sıcaklığı*çözgen oranı gibi iki yönlü değişkenler etkiye sahip değildir. GC-MS sonuçlarına göre ürün dağılımı çözgen tipi ve çözgen oranına göre değişiklik göstermiştir.

TABLE OF CONTENTS

LIST OF FIGURES	viii
LIST OF TABLES	x
CHAPTER 1. INTRODUCTION	1
1.1. The Goal and the Importance of the Study	1
1.2. Definition of Biomass	2
1.3. Structure of Lignocellulosic Biomass	3
1.4. Supercritical Fluids	6
1.5. Biomass Conversion Technologies	8
1.5.1. Thermochemical Conversion Technologies	9
1.5.1.1. Combustion	9
1.5.1.2. Gasification	10
1.5.1.3. Pyrolysis	11
1.5.1.4. Liquefaction	12
1.5.2. Biochemical Conversion Technologies	13
1.5.2.1. Digestion	13
1.5.2.2. Fermentation	14
CHAPTER 2. LITERATURE SURVEY	15
CHAPTER 3. MATERIALS AND METHODS	23
3.1. Chemicals and Material	23
3.2. Experimental Setup	23
3.3. Experimental Procedure	24
3.4. Experimental Design	25
3.5. Structural Carbohydrate Analysis	26
3.5.1. Extraction	27
3.5.2. NDF (Neutral Detergent Fiber) Analysis	27
3.5.3. ADF (Acid Detergent Fiber) Analysis	28

3.5.4. ADL (Acid Detergent Lignin) Analysis	28
3.6. Product Analysis	29
3.6.1. Liquid Product Analysis	29
3.6.2. Solid Product Analysis	29
 CHAPTER 4. RESULTS AND DISCUSSION.....	30
4.1. Effect of Temperature.....	30
4.2. Effect of Solvents and Their Ratio	34
4.3. Effect of Reaction Time.....	37
4.4. Analysis of Variance (ANOVA).....	39
4.5. GC-MS Analysis	44
4.6. FT-IR Analysis	46
 CHAPTER 5. CONCLUSION	49
 REFERENCES	50
APPENDICES	
APPENDIX A. GC-MS DETECTED COMPOUND LIST	55
APPENDIX B. GC-MS CHROMATOGRAMS.....	59

LIST OF FIGURES

<u>Figure</u>	<u>Page</u>
Figure 1.1. Global Production of Hazelnut.....	2
Figure 1.2. General Composition of Lignocellulosic Biomass.....	3
Figure 1.3. Cellulose Structure	4
Figure 1.4. Xylose structure.....	5
Figure 1.5. Lignin monomers	5
Figure 1.6. Structure of lignin.....	6
Figure 1.7. Phase diagram of Ethanol.....	7
Figure 1.8. Phase Diagram of Acetone	8
Figure 1.9. Biomass conversion technologies	9
Figure 1.10. Biomass combustion flowchart	10
Figure 1.11. Pyrolysis and gasification reactions	11
Figure 1.12. Usage areas of liquid intermediates during pyrolysis	12
Figure 1.13. General flowchart of liquefaction.....	13
Figure 1.14. Typical diagram of digestion.....	14
Figure 1.15. Fermentation stages and products	14
Figure 2.1. Effect of solvent on the yields	15
Figure 2.2. Effect of solvent on product distribution.....	16
Figure 2.3. Effects of temperature on yields.....	17
Figure 2.4. Effects of solid/liquid ratio on yields	17
Figure 2.5. Effects of temperature and solvent type on biomass conversion	18
Figure 2.6. Conversion and product yields after liquefaction of cellulose, xylose and lignin in scEtOH as a function of temperature	19
Figure 2.7. Effect of ethanol content on the bio-oil yield, solid residue and other.....	20
Figure 2.8. Effect of temperature on the yields of product fractions	21
Figure 2.9. Effect of A/M ratio on the yields of product fractions	21
Figure 2.10. Effect of time on the yields of product fractions.....	22
Figure 3.1. Thermochemical conversion reactor	24
Figure 4.1. Temperature and solvent effects for hazelnut shell conversion for 30 min reaction time.....	31

Figure 4.2. Temperature and solvent effects for hazelnut shell conversion for 60 min reaction time	32
Figure 4.3. Temperature and solvent effects for hazelnut shell conversion for 90 min reaction time	33
Figure 4.4. Temperature and solvent effects for bio-oil yield for 30 min reaction time	34
Figure 4.5. Temperature and solvent effects for bio-oil yield for 60 min reaction time.....	35
Figure 4.6. Temperature and solvent effect for bio-oil yield for 90 min reaction time.....	36
Figure 4.7. Histogram plots of conversion of hazelnut shell waste.....	40
Figure 4.8. Histogram plots of bio oil yield from hazelnut shell waste.....	40
Figure 4.9. Response surface plot of Bio oil yield from hazelnut shell waste.....	42
Figure 4.10. Response surface plot for the conversion of hazelnut shell waste	43
Figure 4.11. Optimum operating conversion for maximum conversion and maximum bio oil yield	43
Figure 4.12. FT-IR spectrum of untreated and treated hazelnut shell samples at different temperatures	47
Figure 4.13. FT-IR spectrum of treated hazelnut shell samples at different reaction times at 300 °C	48
Figure 4.14. FT-IR spectrum of treated hazelnut shell samples with different ethanol/acetone (v/v) at 300 °C	48

LIST OF TABLES

<u>Table</u>	<u>Page</u>
Table 1.1. Structural carbohydrate distribution of some lignocellulosic biomasses	4
Table 2.1. Effects of temperature and solvent type on biomass conversion.....	18
Table 3.1. Chemicals used in Structural Analysis	23
Table 3.2. Experimental Design of Hazelnut Shell Conversion	25
Table 3.3. Hazelnut Shell Composition	27
Table 4.1. Experimental results of hazelnut shell liquefaction at three different temperatures	30
Table 4.2. Change of biomass conversion and bio-oil yield with respect to time and solvent ratio at 220 °C.....	38
Table 4.3. Change of biomass conversion and bio-oil yield with respect to time and solvent ratio at 260 °C	38
Table 4.4. Change of biomass conversion and bio-oil yield with respect to time and solvent ratio at 300 °C	39
Table 4.5. Statistical analysis results of hazelnut shell conversion and bio oil yield (non-reduced model)	41
Table 4.6. Statistical analysis results of hazelnut shell conversion and bio oil yield (reduced model).....	41

CHAPTER 1

INTRODUCTION

Interests on the alternative and renewable resources have been improved as a result of the gradual depletion of fossil fuels, the world's population growth, increasing greenhouse gas emission and climate change.¹⁻⁵ Currently, both energy and chemical necessities have supplied from nonrenewable sources such as coal and petroleum. Usage of solar, wind, energy is growing day by day to compensate energy demand. In addition to that, these energy sources are cheap, renewable and have less carbon footprint compared to nonrenewable energy sources.⁶⁻⁷ Utilization of biomass has big potential among all renewable sources since it is abundant, almost carbon neutral process.⁸ Also, solid, liquid and gaseous products can be produced from biomass that is only renewable carbon source. Carbon dioxide is released while production of fuels, chemicals, heat and power from biomass. However, this released carbon dioxide has already captured via photosynthesis. Therefore, biomass utilization is significantly important to produce value-added chemicals, bio-oils or bio-fuels. Furthermore, waste lignocellulosic biomass attracts more attention as a raw material due to the fact that it is not preferred for nutritional needs.⁶⁻⁷ On the other hand, many efforts have been made to utilize lignocellulosic biomass better through thermochemical processes. Gasification⁹, pyrolysis¹⁰, direct combustion¹¹, liquefaction¹², and hydrothermal electrolysis¹³ constitutes thermochemical processes.

1.1. The Goal and the Importance of the Study

The goal of this study is to examine the potential of waste hazelnut shell as a raw material for the production of bio-oil since Turkey dominates the global production of hazelnut in the world as it can be seen Figure 1.1. The other aim is to determine the product distribution and optimum process parameters such as reaction temperature (220-300 °C), reaction time (30-90 min), solvent ratio (0-100) to reach the highest bio-oil yield. In literature, there is no study about production of bio-oil from hazelnut shell waste by using sub/supercritical ethanol, acetone and their mixture as reaction medium.

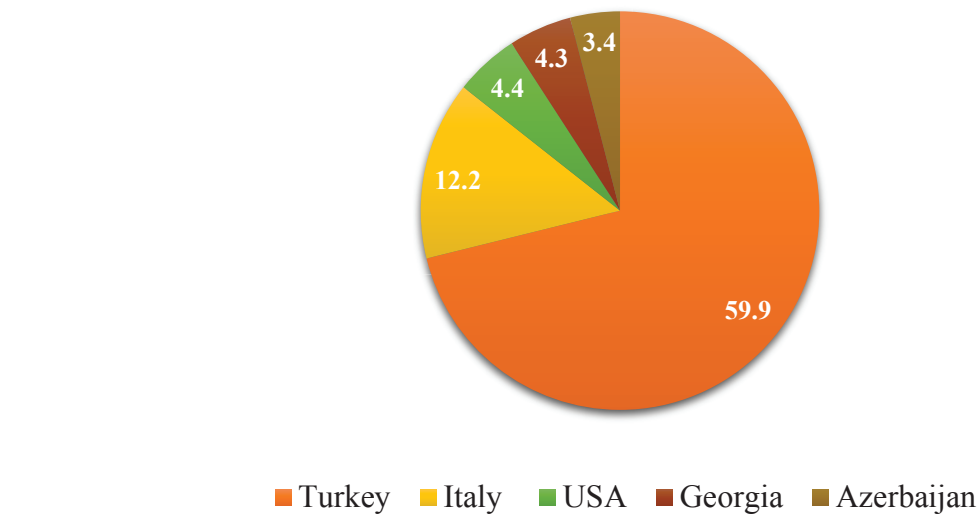


Figure 1.1. Global Production of Hazelnut
(Source: FAOSTAT, 2016)

Ethanol and acetone are chosen since supercritical alcohols have some more benefits than subcritical water as a solvent in the direct liquefaction of biomass.¹⁴⁻¹⁸ These benefits consist of better solubility of biomass and its intermediates, much easier product separation, having lower corrosivity, hydrogen donation ability and showing higher bio-crude/bio-oil yield.¹⁴ The dominant mechanism in subcritical hydrothermal liquefaction includes hydrolytic and pyrolytic cleavage, whereas for supercritical ethanol-based liquefaction main degradation mechanism follows only pyrolytic cleavage. Acetone, on the other hand, is a dipolar aprotic solvent and shows different polarity than ethanol. It is one of the most used organic solvents in extraction and cleaning purposes, and there is very limited work in literature about using acetone as a sub/supercritical fluid in biomass liquefaction.¹⁹ The other thing is that behavior of acetone and ethanol ratio in product distribution do not studied before in the literature.

1.2. Definition of Biomass

Biomass is a biological matter that contains both flora and fauna. Biomass resources include wood and wood waste, agricultural crops, aquatic plants, energy crops and animal wastes.²⁰ CO₂ in the air, water and sunlight are reacted with each other to form the carbohydrates during the photosynthesis. The solar energy from the sunlight is stored in the chemical bonds between carbon, hydrogen and oxygen molecules.⁷ This stored

chemical energy is released by bond breakage with biological and chemical processes. Oxygen molecule oxidizes the carbon in carbohydrate products to produce carbon dioxide and carbon dioxide is reabsorbed by another biomass.²¹ Thus, these biomass types are generally called as sustainable and renewable organic substances. Biomass conversion processes are determined due to biomass type. In other words, while combustion and pyrolysis are suitable for a dry biomass, fermentation is preferred for high moisture content biomass.²²

1.3. Structure of Lignocellulosic Biomass

Lignocellulosic biomass is composed of cellulose, hemicellulose, lignin and small portion of inorganic substances. Composition of lignocellulosic biomass can be seen in Figure 1.2.

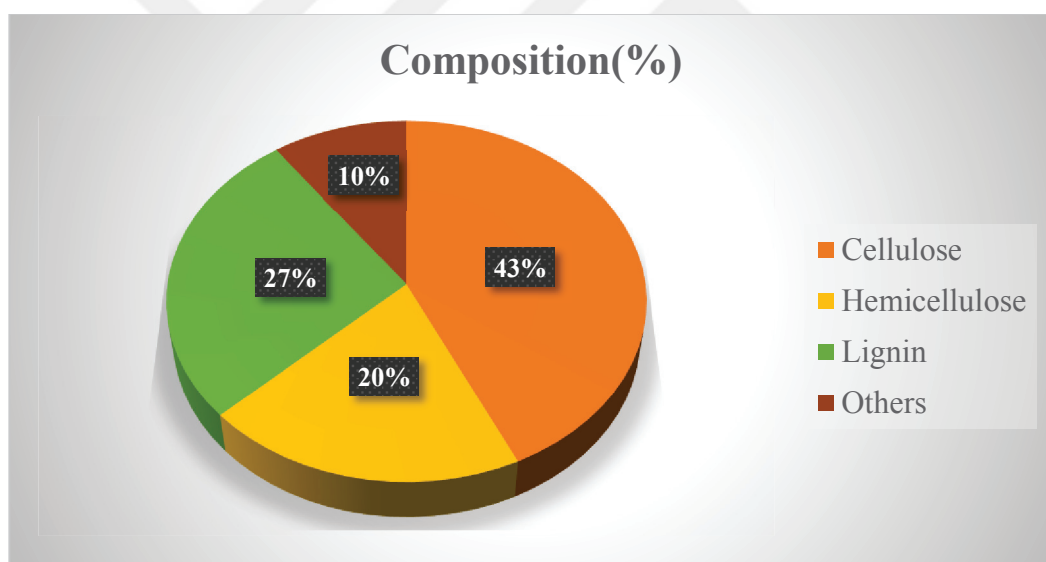


Figure 1.2. General Composition of Lignocellulosic Biomass

This heterogeneous mixture composition changes with many factors such as growth stage, biomass type, tissue type and growing conditions. The structural carbohydrate distribution of some lignocellulosic biomasses is listed in Table 1.1. Cellulose and hemicellulose are the carbohydrate part, whereas lignin forms the non-carbohydrate part of the biomass. The Structural and mechanical strength in the biomass comes from cellulose and hemicellulose. Lignin, on the other hand, provides the stability of cellulose, hemicellulose.

Table 1.1. Structural carbohydrate distribution of some lignocellulosic biomasses
(Source Fang and Xu, 2014)

Biomass	Cellulose (wt.%)	Hemicellulose (wt.%)	Lignin (wt.%)
Tobacco leaf	43.45	41.54	15.01
Corncob	52.49	32.32	15.19
Corn straw	51.53	30.88	17.59
Wheat straw	33.82	45.20	20.98
Beech wood	46.27	31.86	21.87
Hardwood	45.85	32.26	21.89
Softwood	42.68	24.82	32.50
Spruce wood	47.11	21.31	31.58
Hazelnut shell	26.70	30.29	43.01
Wood bark	25.59	30.28	44.13
Olive cake	23.08	21.63	55.29

Cellulose is a long linear chain polymer of glucose with a degree of 1,000- 10,000. Glucose molecules bonds each other with β -1,4-glycocidic linkages as it can be seen in Figure 1.3. Cellulose can be amorphous and crystalline. Hydrogen bonds that are located between chains provides chemical stability and insolubility and also forms structure of plant wall. The reason why cellulose has much more resistance to acid and enzymatic hydrolysis than starch is high degree of crystallinity. Additionally, cellulose is protected from environmental exposure by lignin and hemicellulose.

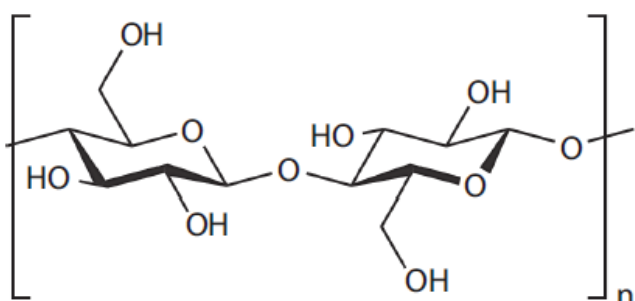


Figure 1.3. Cellulose Structure
(Source: Sengupta and Pike 2013)

Hemicellulose contains five carbon sugars like xylose and arabinose with glucose and mannose. Xylose structure is shown in Figure 1.4. It is formed from short-chain polymer and it interacts with cellulose and lignin to create a matrix in the plant wall. This matrix gives the strength to plant cell wall. Hydrolysis of hemicellulose is easier than cellulose. Big portion of hemicellulose in lignocellulosic materials decomposes to

pentose and hexose sugars by solubilization and hydrolysis during the pretreatment stage. Small portion of hemicellulose is intertwined with the lignin.

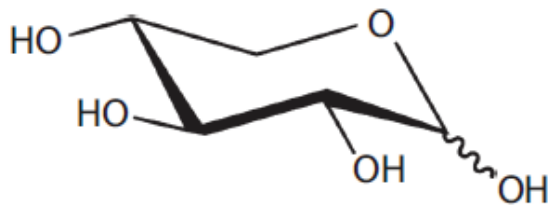


Figure 1.4. Xylose structure
(Source: Sengupta and Pike 2013)

Lignin is formed randomly and disorganized ring-structured polymers such as benzene rings with methoxyl, propyl and hydroxyl functional groups Figure 1.6. These functional groups bind each other aryl-ether linkages with aryl-glycerol- β -aryl ether and with the help of this both binding cellulose/hemicellulose matrix and flexibility of the mixture. On the other hand, lignin has great potential to produce valuable chemical intermediates majorly aromatic components because of ring structured monomers. It is hard to break down lignin bonds without using further chemicals. Acid treatments may be shown an option but concentrated sulfuric acid decomposes cellulose, hemicellulose and lignin matrix while lignin is not soluble in sulfuric acid. The only small amount of lignin can be dissolved by acid addition to reaction. Furthermore, pyrolysis can be used to produce value added chemicals from lignin polymers but still separation is a problem. Therefore, lignin is fractionated to high phenolic content bio-oil for production of bio-fuel and phenol-formaldehyde resins. In addition to that, lignin has higher energy content compared with cellulose and hemicellulose. This means that, increasing lignin composition in the biomass provides higher heating values.

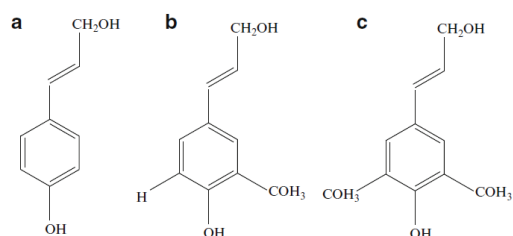


Figure 1.5. Lignin monomers a) trans-p coumaryl alcohol, b) coniferyl alcohol, and c) sinapyl alcohol (Source: Lee 2013)

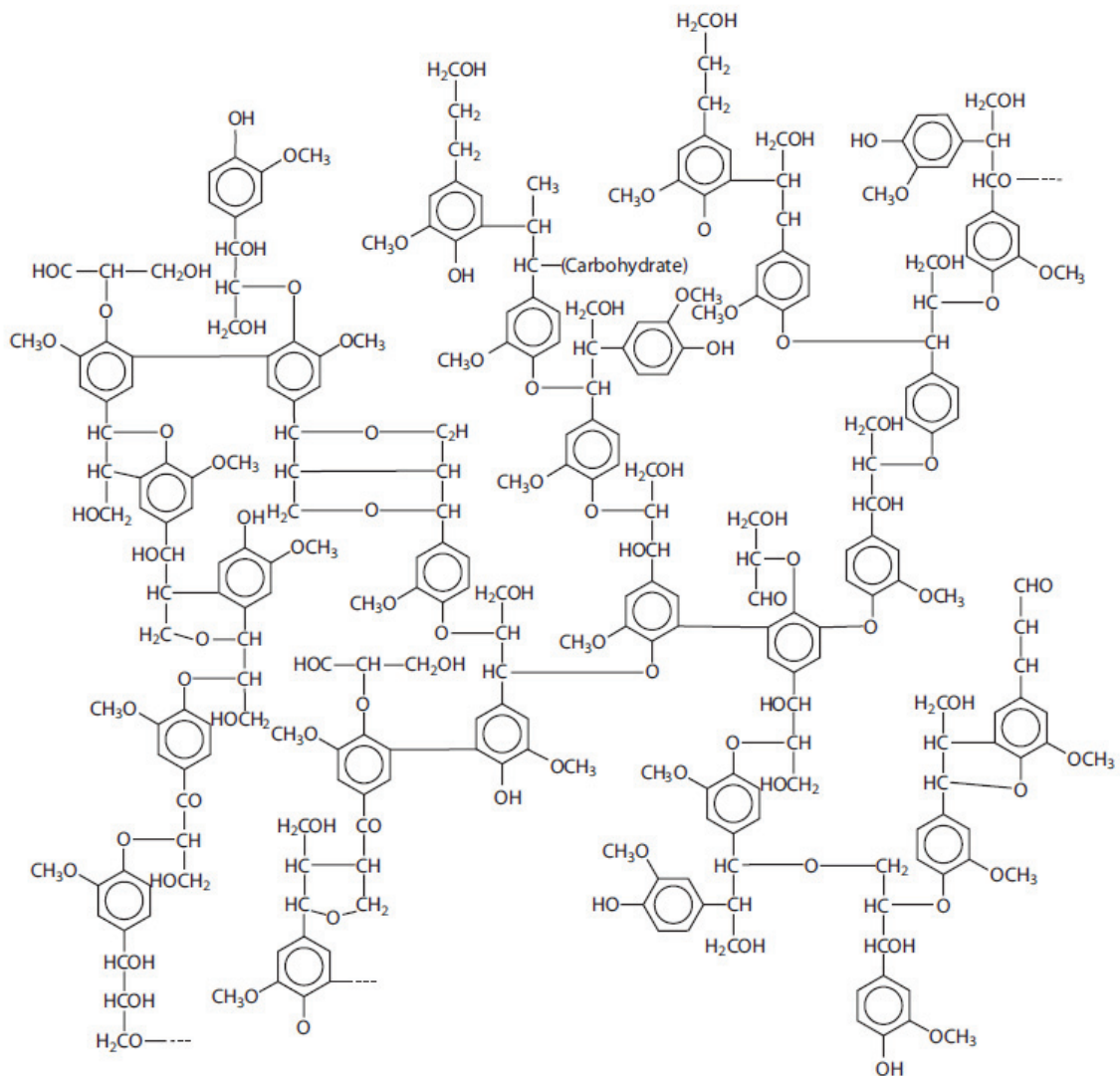


Figure 1.6. Structure of lignin
(Source: Glazer and Nikaido 1995)

1.4. Supercritical Fluids

In order to understand what the supercritical fluid is, firstly we have to understand subcritical fluid. Subcritical fluid can be defined as fluid is compressed after its boiling point until critical point. In subcritical region, fluid is liquid state. In subcritical region, fluids tend to give proton due to its nature. Therefore, ionic reactions are more dominant in reaction mechanism.

Supercritical fluid is a fluid that temperature and pressure of the fluid above its critical temperature and pressure. In supercritical region, substances act like both gas and liquid. However, there is no phase separation because of no surface tension. Additionally,

supercritical fluids can effuse through solids as a gas, and dissolve them as a liquid. On the other hand, properties of supercritical fluids can be set by changing temperature or pressure as more liquid like or gas like. Having a high density is a sign of liquid-like property, whereas high diffusivity and low viscosity refers to the gas-like properties. High density is responsible for high solving power of the liquid, while high diffusivity and low viscosity are in charge of controlling mass transfer rates of reactants. That leads to, diffusion limited reactions enhancement in sub/supercritical fluids with respect to liquids.²³ Some of the physical properties like dielectric constant, viscosity, and thermal conductivity are functions of density. In other words, when density changes these properties also change. All supercritical fluids can be dissolved within each other. It is guaranteed that when a mixture in supercritical region, there will be only single phase. In addition to all, in supercritical region reaction rate and reaction mechanisms increase. While ionic reactions are most dominant reactions at low temperatures, at high temperatures radical reactions are more. It is because of homolytic bond breakage.²⁴ The phase diagrams of ethanol and acetone were given in Figure 1.7 and Figure 1.8, respectively.

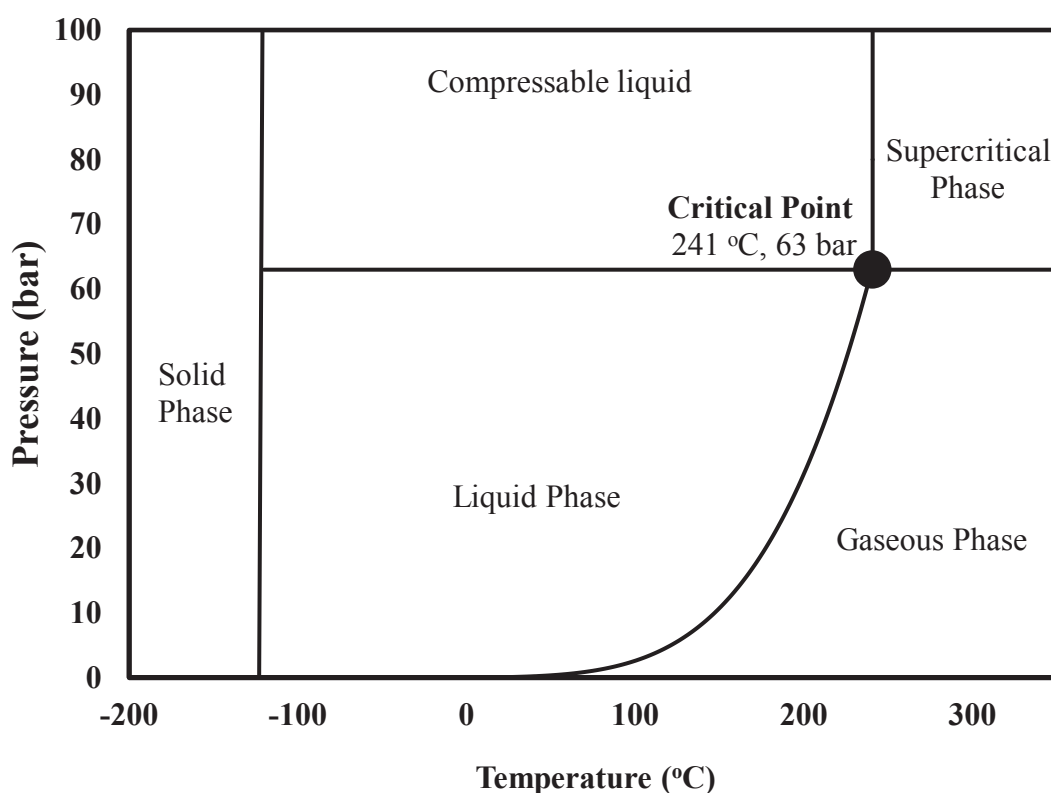


Figure 1.7. Phase diagram of Ethanol

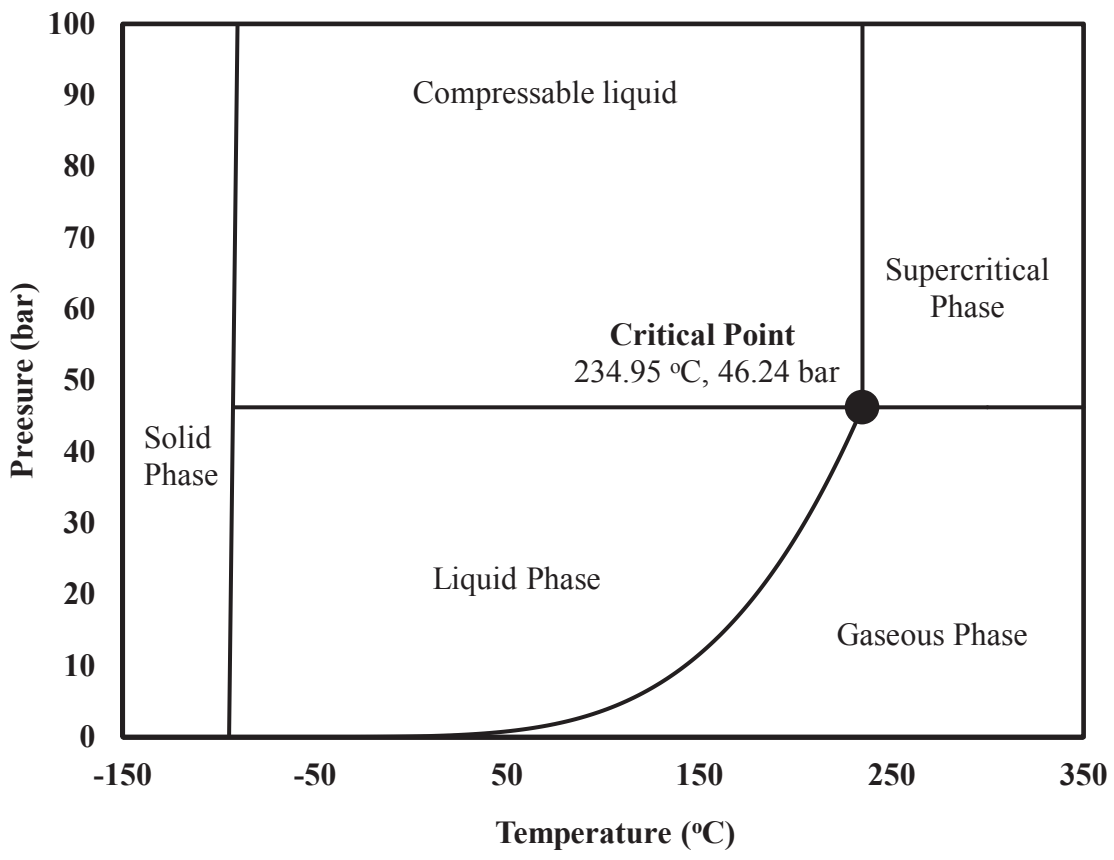


Figure 1.8. Phase Diagram of Acetone

1.5. Biomass Conversion Technologies

There are many conversion processes to convert biomass into valuable chemicals, fuels and heat/power. Selection criteria changes with several factors;

- Biomass type
- Environmental issues
- Objective use
- Economic and social concerns

Biomass conversion technologies can be classified in two major groups. These are thermochemical and biochemical conversion. Thermochemical conversion identifies thermal bond breakage of structures in biomass while biochemical conversion identified enzymatic breakdown of biomass. In more detail, biomass conversion technologies can be seen Figure 1.9.

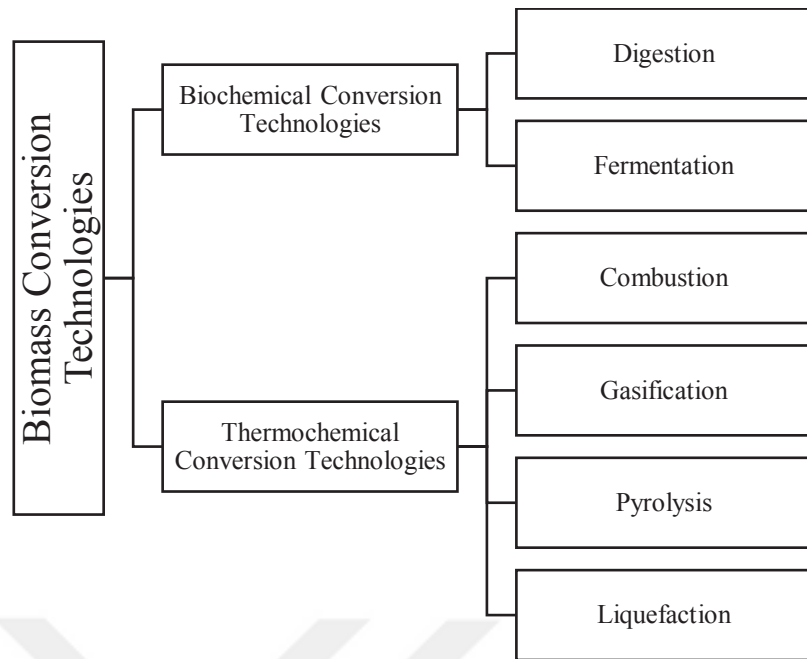


Figure 1.9. Biomass conversion technologies

1.5.1. Thermochemical Conversion Technologies

Thermochemical processes are best known technologies by humankind. Basically, it can be said thermal break down of bonds in the biomass.²⁵ Thermochemical processes are mostly used in the conversion of biomass to fuels that have higher heating value. There are a lot of studies in literature about thermochemical technologies to produce valuable chemicals, fuel and heat/power. Thermochemical technologies are consisted of combustion, gasification, pyrolysis, liquefaction.⁶

1.5.1.1. Combustion

Combustion is the best-known process after the discovery of controlled fire. Biomass is burned in the presence of air. In general, stored energy in chemical bonds of lignocellulosic biomass is converted to heat and this heat can be converted to mechanical power with steam. This steam is used in steam turbines to produce electricity. After combustion of biomass preferably low moisture content, temperature of produced hot gases is between 800-1000 °C. Actually, combustion reactions are complicated but majorly it can be classified devolatilization and char combustion. This mechanism can be

seen from Figure 1.10. The volatile hydrocarbons, carbon monoxide and hydrogen are formed during the volatilization and they produce more heat energy by oxygen. Produced heat is converted to electricity by boilers, turbines and burners. Biomass like forest residue, sawdust pellets, municipal waste can be used in combustion. Normally, combustion is classified pollutant process due to production of nitrogen oxides and sulfur oxides. Nevertheless, combustion of biomass is carbon neutral process.²⁵

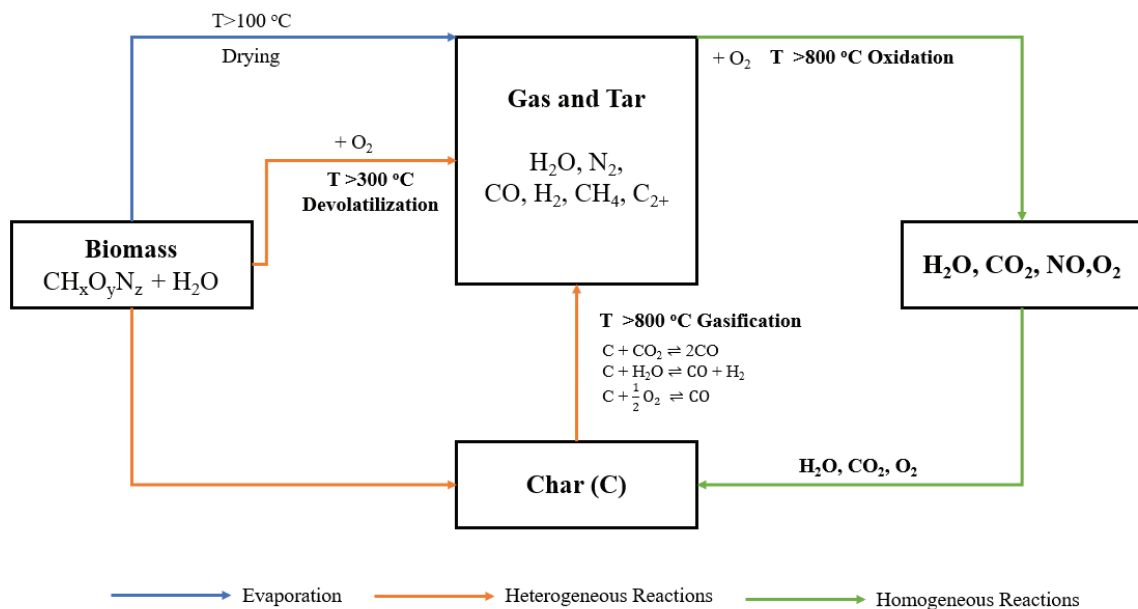


Figure 1.10. Biomass combustion flowchart
(Source: Nussbaumer 2003)

1.5.1.2. Gasification

Gasification is a process that biomass is converted to synthesis gases such as hydrogen and carbon monoxide by partial oxidation of biomass by using oxidizing agent like oxygen, ethanol, supercritical water. Gasification process is carried out at higher temperature range $700\text{-}1000^\circ\text{C}$ with higher gas yields formation up to 85%. Gasification steps are affected by moisture content of biomass if biomass is dried in the reactor. In order to dry biomass water will have latent heat of vaporization and this means much energy is required. As a result of this, biomass moisture content must be controlled. As fuel temperature increases to range of $200\text{-}700^\circ\text{C}$, pyrolysis takes place in the absence of air or oxygen. In this stage, condensable hydrocarbon tars, oils, methane and char

formation occurs. As bond breakage continues, hydrogen is formed and reacts with oxygen. As a result of this reaction water is formed. The pyrolysis stage is endothermic process and this stage requires energy to drive pyrolysis to partial combustion in the gasifier.²⁵ Pyrolysis and gasification stage reactions are shown in Figure 1.11.

$C + \frac{1}{2}O_2 \rightleftharpoons CO$	$\Delta H_r^\circ = -111 \text{ kJ.mol}^{-1}$
$H_2 + \frac{1}{2}O_2 \rightarrow H_2O$	$\Delta H_r^\circ = -242 \text{ kJ.mol}^{-1}$
$CO + \frac{1}{2}O_2 \rightarrow CO_2$	$\Delta H_r^\circ = -283 \text{ kJ.mol}^{-1}$
$NH_3 + \frac{3}{4}O_2 \rightarrow \frac{1}{2}N_2 + \frac{3}{2}H_2O$	$\Delta H_r^\circ = -383 \text{ kJ.mol}^{-1}$
$H_2S + \frac{3}{2}O_2 \rightleftharpoons SO_2 + H_2O$	$\Delta H_r^\circ = -563 \text{ kJ.mol}^{-1}$
$C + CO_2 \rightleftharpoons 2CO$	$\Delta H_r^\circ = +172 \text{ kJ.mol}^{-1}$
$C + H_2O \rightleftharpoons CO + H_2$	$\Delta H_r^\circ = +131 \text{ kJ.mol}^{-1}$
$CO + H_2O \rightleftharpoons H_2 + CO_2$	$\Delta H_r^\circ = -41 \text{ kJ.mol}^{-1}$
$CH_4 + H_2O \rightleftharpoons 3H_2 + CO$	$\Delta H_r^\circ = +210 \text{ kJ.mol}^{-1}$
$NH_3 \rightleftharpoons \frac{1}{2}N_2 + \frac{3}{2}H_2$	$\Delta H_r^\circ = +46 \text{ kJ.mol}^{-1}$
$SO_2 + 3H_2 \rightleftharpoons H_2S + 2H_2O$	$\Delta H_r^\circ = +207 \text{ kJ.mol}^{-1}$

Figure 1.11. Pyrolysis and gasification reactions

1.5.1.3. Pyrolysis

Pyrolysis is the direct decomposition of organic compounds to solid, liquid and gaseous components in the absence of oxygen in the range of 300-600 °C. During the pyrolysis, formed solid product is called as biochar or charcoal. This solid product contains 85% pure carbon. The liquid product includes organic acids, furfurals and phenolic components and dominant gaseous products are CO, CO₂, CH₄ and H₂. Liquid product distribution highly depends on temperature. Cost effective process is required for separation of these intermediates. Usage areas of these intermediates are shown in Figure 1.12. Pyrolysis is diverged to two groups: Slow pyrolysis and fast pyrolysis. Slow pyrolysis requires low temperature, high residence time and slow heating rate to produce biochar whereas fast pyrolysis requires higher temperature and short residence and high heating rate to produce mostly bio-oil.²¹⁻²²

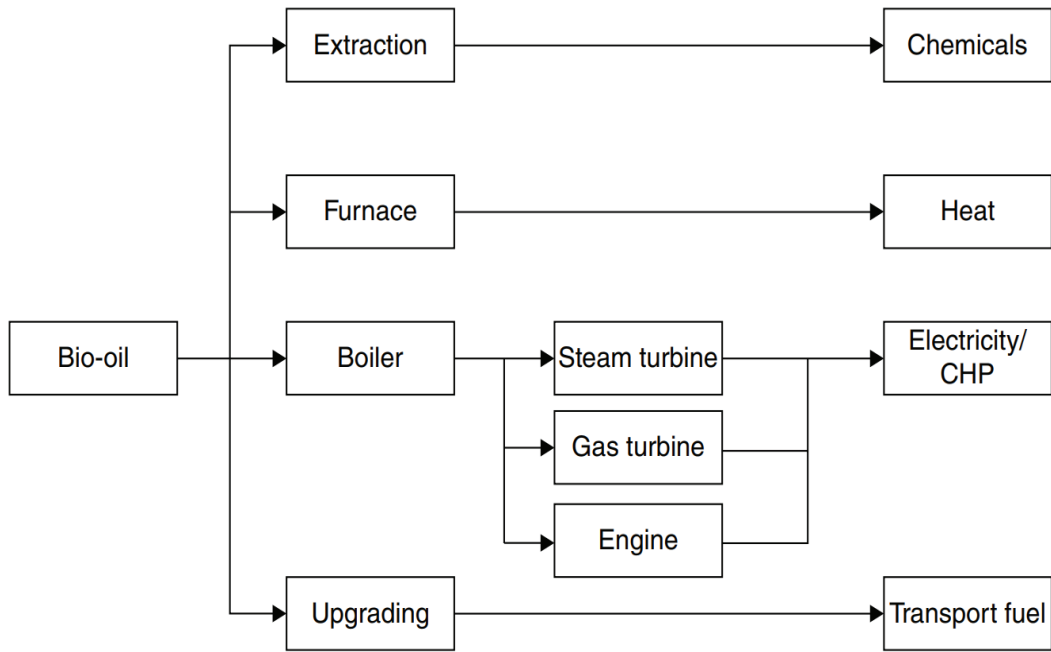


Figure 1.12. Usage areas of liquid intermediates during pyrolysis
 (Source: Clark and Deswarte 2015)

1.5.1.4. Liquefaction

Liquefaction is conducted at high pressures (50-300 bar) and low temperatures (200-400 °C) compared with gasification, combustion and pyrolysis in aqueous medium. General flowchart of liquefaction is given Figure 1.13. All kind of biomass type can be used in liquefaction; for instance, wood, agricultural waste, algae, municipal waste etc. Liquefaction has some advantages compared with pyrolysis such that low oxygen content. This low oxygen content provides higher energy density. Produced bio-oil is more vicious than crude oil. Bio-oils can include up to 400 compounds. Distribution of compounds highly depend on reaction conditions. This bio-oil can be used as heavy petroleum oil replacement.²²

Firstly, feed stock is pumped by appropriate pump type to heat exchanger to rise solvent temperature. After heating, this solvent goes to reactor. In reactor, solvent and reactants react with each other in a certain time. Completed reaction products go to the cooler to decrease the temperature of medium. In this section, pressure of the products is smaller than before the cooler. Therefore, pressure of this mixture must be decrease further in pressure reduction unit. The last part of the liquefaction is separation. In this section, oil is separated from the mixture by using different separation technique.

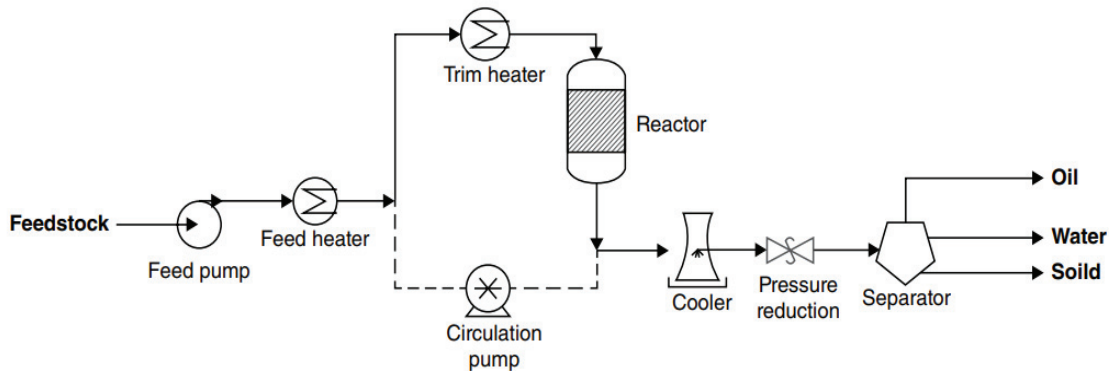


Figure 1.13. General flowchart of liquefaction
(Source: Clark and Deswarte 2015)

1.5.2. Biochemical Conversion Technologies

Biochemical conversion can be divided into two groups: Fermentation and digestion. These techniques are generally carried out by using enzymes and microorganisms to produce bio-ethanol as a liquid product and bio-gas as a gaseous product.

1.5.2.1. Digestion

Digestion is conversion of organic material into gaseous products. These gaseous products are composed of methane, carbon dioxide and small amount of hydrogen sulfide. During the digestion microorganisms like methanogenic, acetogenic bacteria, fermentative bacteria are used. Digestion includes four stages that are hydrolysis, acidogenesis, acetogenesis and methanogenesis. Insoluble organic compounds are converted to soluble compounds by using hydrolases. After hydrolysis, soluble compounds turn to organic acids, aldehydes, alcohol, hydrogen and carbon dioxide during acidogenesis. Moreover, process continues to produce carbon dioxide, hydrogen and acetates with in acetogenesis part. Methanogenesis bacteria produce methane at the last stage of digestion. Final gaseous mixture can be directly used in combustion chambers due to its composition. Substrate composition determines the composition of gaseous mixture. While lipids give the highest methane yield as $1014 \text{ m}^3 \text{ ton}^{-1}$, proteins and carbohydrates do not give as high as lipids $415\text{--}496 \text{ m}^3 \text{ ton}^{-1}$.²¹ A typical diagram of digestion is shown in Figure 1.14.

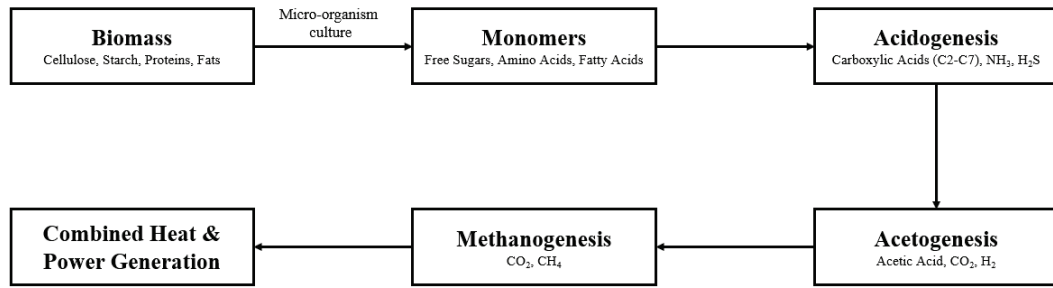


Figure 1.14. Typical diagram of digestion
(Source: Sengupta and Pike 2013)

1.5.2.2. Fermentation

Fermentation is a process that converts sugars into biofuels, biochemicals or bio compounds by using microorganisms. Fermentation is commercially proven technology in large scales. It is generally used to produce bio ethanol from sugar crops (sugar beet, sugarcane, switchgrass) as feedstock. However, lignocellulosic biomasses are not directly used in fermentation due to long-chain polysaccharides. Acid and enzymatic treatment is needed to obtain fermentable sugars.²⁶ Fermentation stages are given in the Figure 1.15

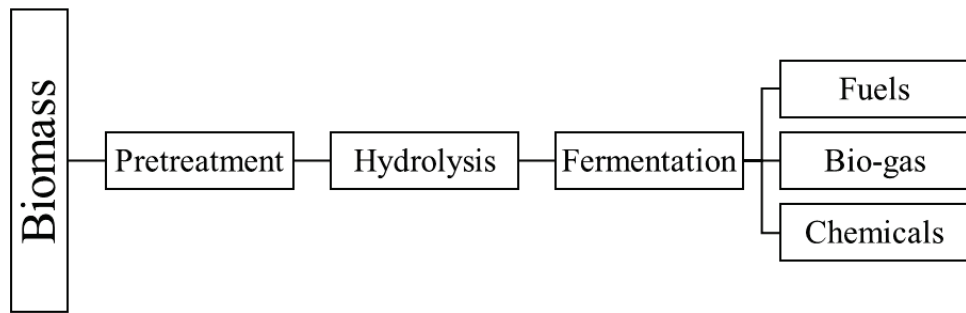


Figure 1.15. Fermentation stages and products

CHAPTER 2

LITERATURE SURVEY

Effects of different solvents (acetone, ethanol, ethylene glycol, toluene and water) on the liquefaction of oil palm empty fruit brunch fibers study can be given as example in the literature.²⁷ They observed that best solid conversion and bio-oil yield with ethylene glycol as and lowest conversion and bio-oil yield was observed with toluene as a solvent Figure 2.1.

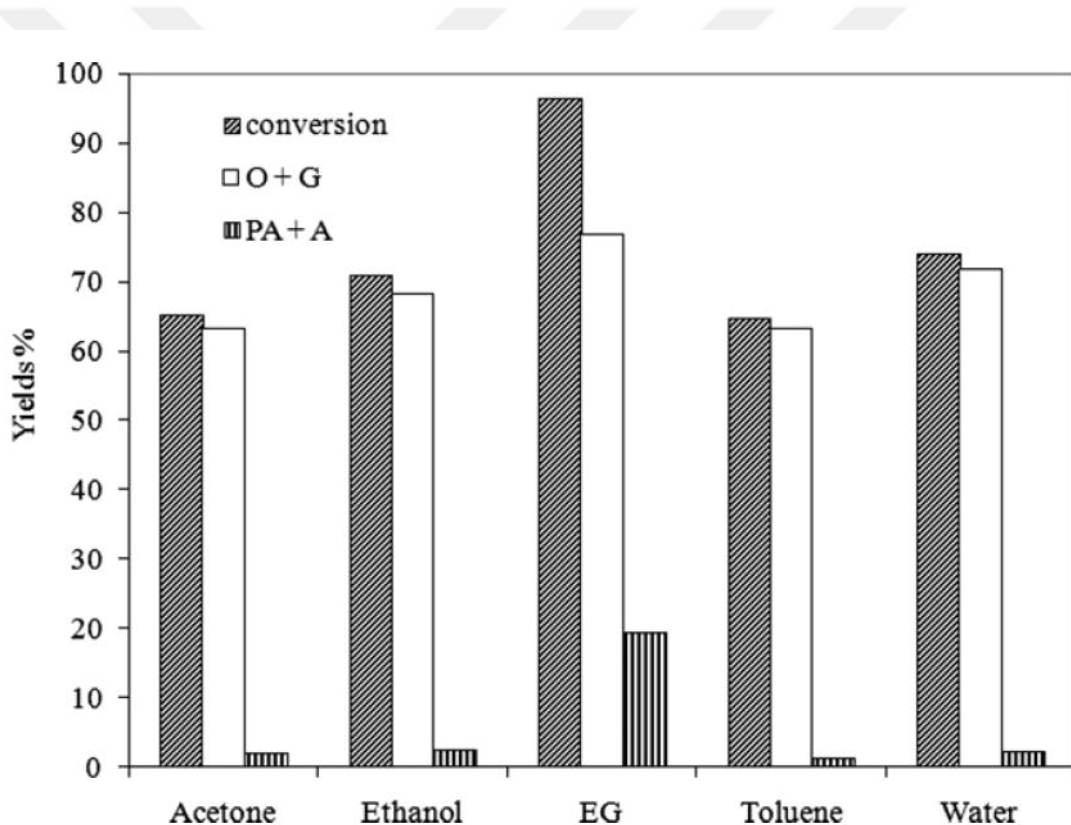


Figure 2.1. Effect of solvent on the yields
(Source: Fan et al. 2011)

Furthermore, product distribution changes with respect to solvent type Figure 2.2. Ethylene glycol has majorly produced alcohol derivatives. This is because of degradation of cellulose initially to organic acids and these acids were hydrolyzed to alcohol derivatives. Phenolic components were observed in water, ethanol and toluene. These phenolics were originated by low molecular weight of lignin that is dehydration of -OH

groups in the alkyl chain in lignin structure. Simplest product distribution, mostly phenols, was obtained by using water as a solvent.

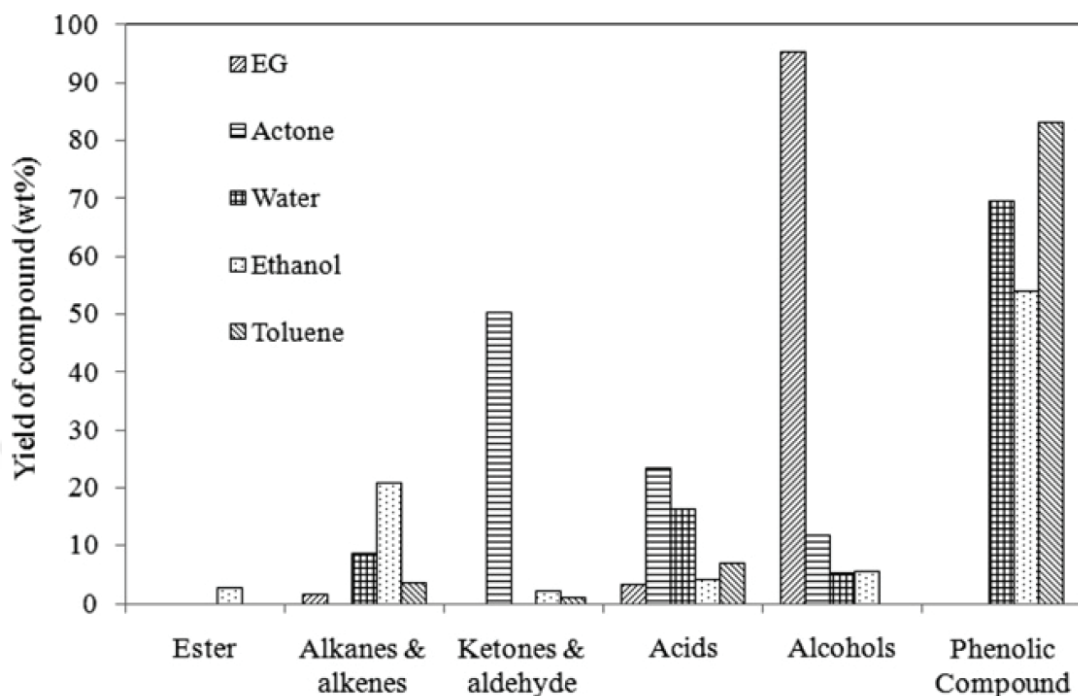
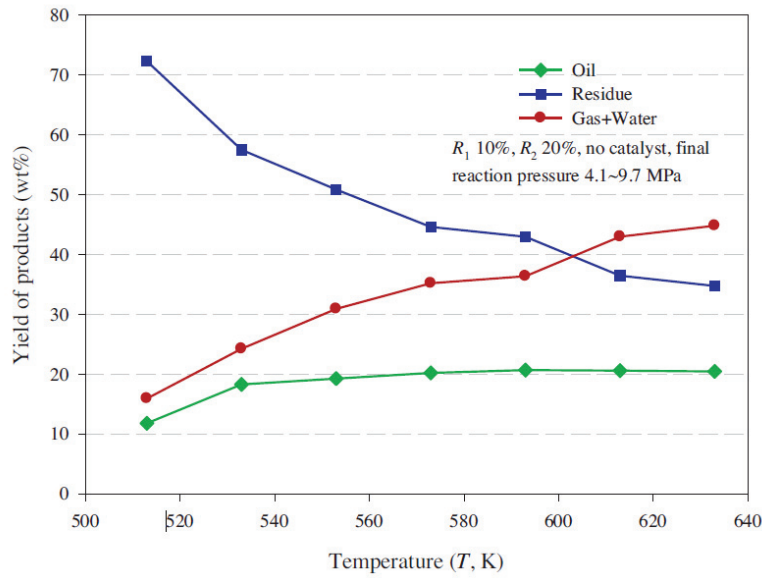


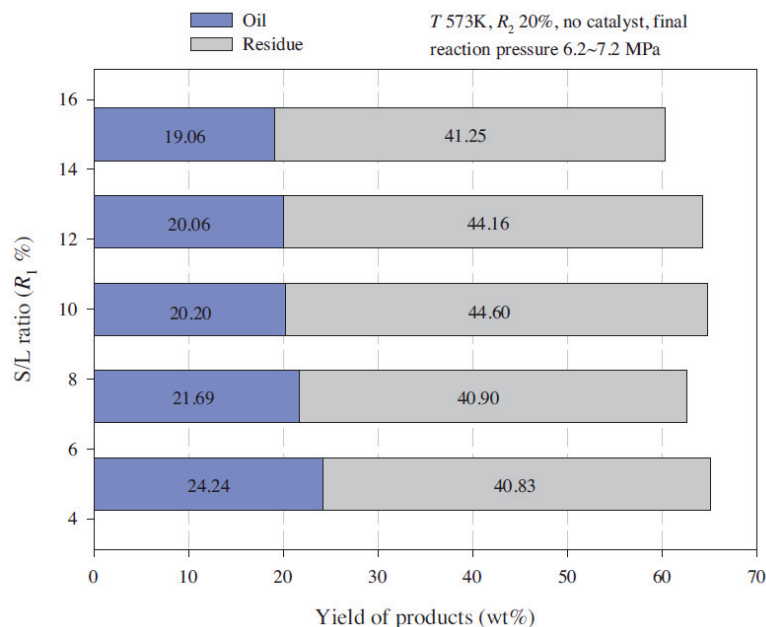
Figure 2.2. Effect of solvent on product distribution
(Source: Fan et al. 2011)

In another work, researchers investigated the thermochemical liquefaction of rice husk in sub/supercritical ethanol. In that study, different temperatures (240-360 °C) and solid liquid ratios (5-15%) was investigated as parameters.²⁸ They observed that bio-oil yield does not increase after 280 °C, whereas gas product percentage was continuing to increase. Additionally, solid conversion increases with increasing temperature as it can be seen in Figure 2.3. Furthermore, Bio-oil yield is remaining constant and increasing gas yield since boudouard gas reactions are dominant at high temperatures.

They obtained that increasing solid Solid/Liquid ratio (5-15%) was resulted with decreasing bio-oil yield as can be seen in Figure 2.4. Because during liquefaction process, biomass components are extracted and break down by solvent to reaction medium. At high solid/liquid ratios, solvent and biomass interactions are relatively low compared with low solid/liquid ratios. In other words, solubility of components was weakened in solvent. Solvent provides stability and solubility of fragments in the reaction medium. Hence, bio-oil yield decreases with increasing solid/liquid ratio as expected (from 24.24% to 19.06%).



In other words, solubility of components was weakened in solvent. Solvent provides stability and solubility of fragments in the reaction medium. Hence, bio-oil yield decreases with increasing solid/liquid ratio as expected (from 24.24% to 19.06%). Therefore, critical S/L must be calculated to get best bio-oil yield. Also, it can cause more gas compounds formed. In other words, process tend to behave pyrolysis with increasing Solid/ Liquid ratio.



The effects of different solvents (water, acetone and ethanol) and temperature (250-450 °C) on biomass conversion, bio-oil yield were examined in another study.²⁹ Biomass conversion (Figure 2.5) was increased by increasing temperature to 350 °C in all individual solvents. After 350 °C conversion rate decreases in water and acetone. In contrast, biomass conversion increases ethanol for along the temperature range. This is because of low polarity of water after the critical point. In literature there is no polarity data for acetone at critical points. However, general opinion is that polar components tend to behave nonpolar after they reach critical points, whereas nonpolar components tend to be more polar.

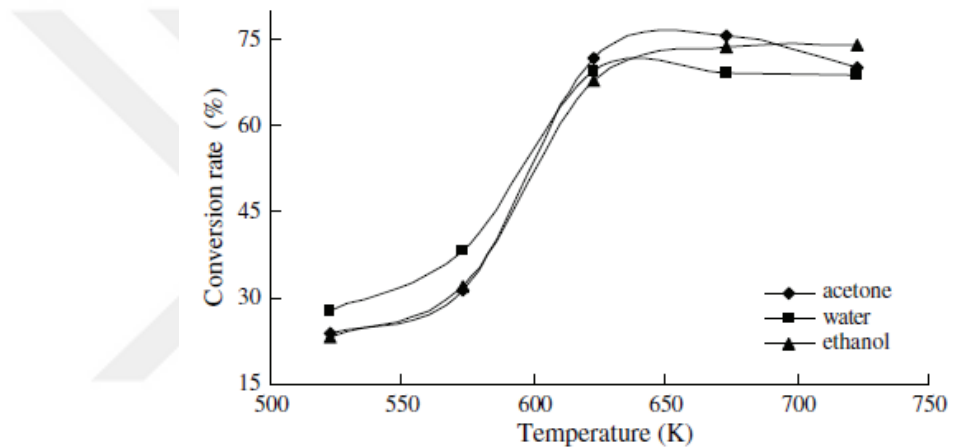


Figure 2.5. Effects of temperature and solvent type on biomass conversion
(Source: Liu and Zhang 2008)

Best bio-oil yield (Table 2.1) was observed at 573 K for water and 673 K for ethanol and acetone as 18.6%, 26.5%, 20.0% respectively. The reason why bio-oil yield decreases after certain temperature that formation of solid by cyclization, re-polymerization, condensation occurred.

Table 2.1. Effects of temperature and solvent type on biomass conversion.
(Source: Liu and Zhang 2008)

	Temperature (K)				
	523	573	623	673	723
	Bio-oil Yield (wt.%)				
Acetone	7.6	10.3	16	20	19.3
Water	10.3	18.6	17.4	16.2	7.1
Ethanol	6.3	13.7	21.5	26.5	19.5

There is a remarkable contribution to understand effect of individual lignocellulosic biomass constituents in supercritical ethanol and made a to the literature.³⁰ Cellulose, hemicellulose (xylose) and lignin were investigated individually by using ethanol Figure 2.6. Lignin conversion was almost steady and not changing in the entire range of temperature they worked (between 290-350 °C), while almost all xylose conversion was finished at the temperature of 260 °C and cellulose conversion was still increasing at around 350 °C by showing around 95% conversion at that point. Furthermore, Bio-oil yield is generated by cellulose, mostly and for cellulose bio-oil yield continues to rise. In spite of that bio-oil yield decreases in temperature range for lignin liquefaction. Although almost all xylose is converted in temperature range, change in bio-oil and gaseous product yields were not significant.

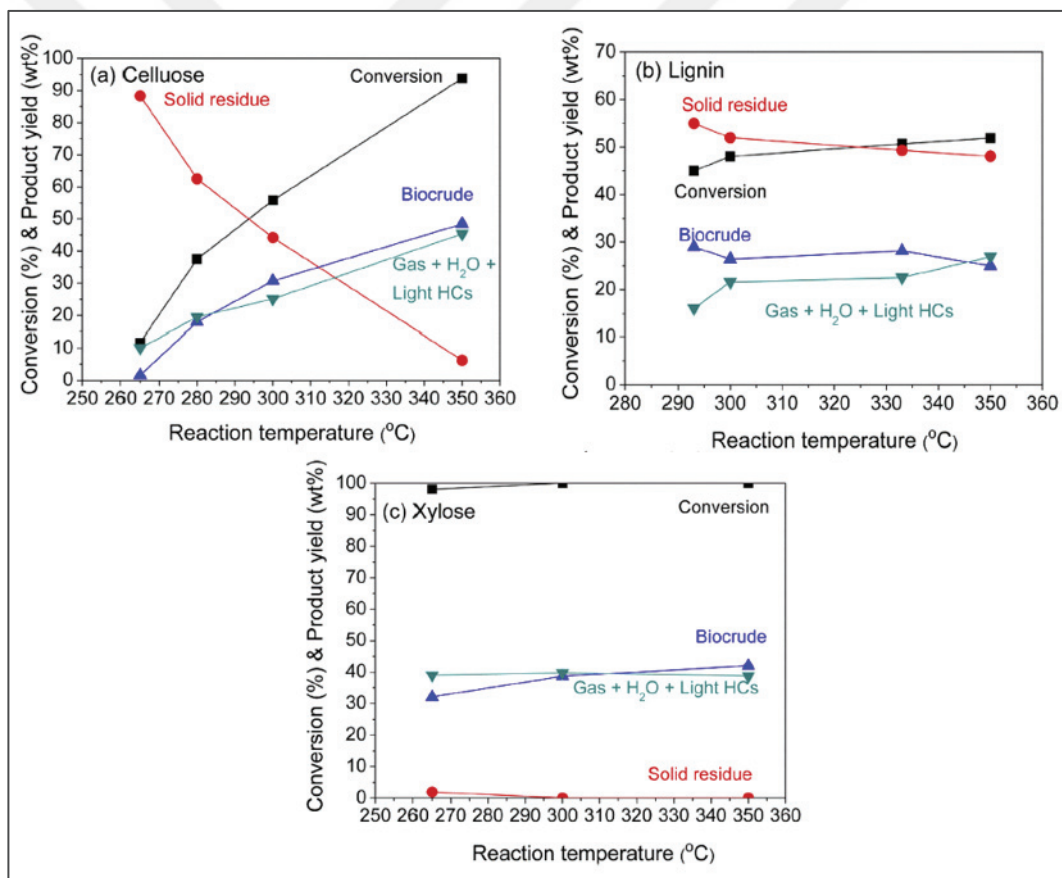


Figure 2.6. Conversion and product yields after liquefaction of cellulose, xylose and lignin in scEtOH as a function of temperature. (Source: Brand and Kim 2015)

In another study investigates effects of ethanol water mixture ratio (0-100 v/v%) on bio-oil yield.³¹ They observed that using pure ethanol or water as a reaction medium has low effect on conversion and bio-oil yield compared with ethanol-water mixtures.

Ethanol and water mixtures showed synergistic effect on conversion and bio-oil yield. The highest bio-oil yield and conversion were reached with the 40 % v/v ethanol/water mixture Figure 2.7. However, increasing ethanol amount was resulted with decrement of bio-oil yield. This can be explained by decreasing critical temperature of mixture. When ethanol amount is 40% v/v, critical temperature of ethanol in the mixture 326 °C while liquefaction temperature is 320 °C. Therefore, increment of ethanol amount resulted with decrease of critical temperature and pressure of ethanol in the mixture.

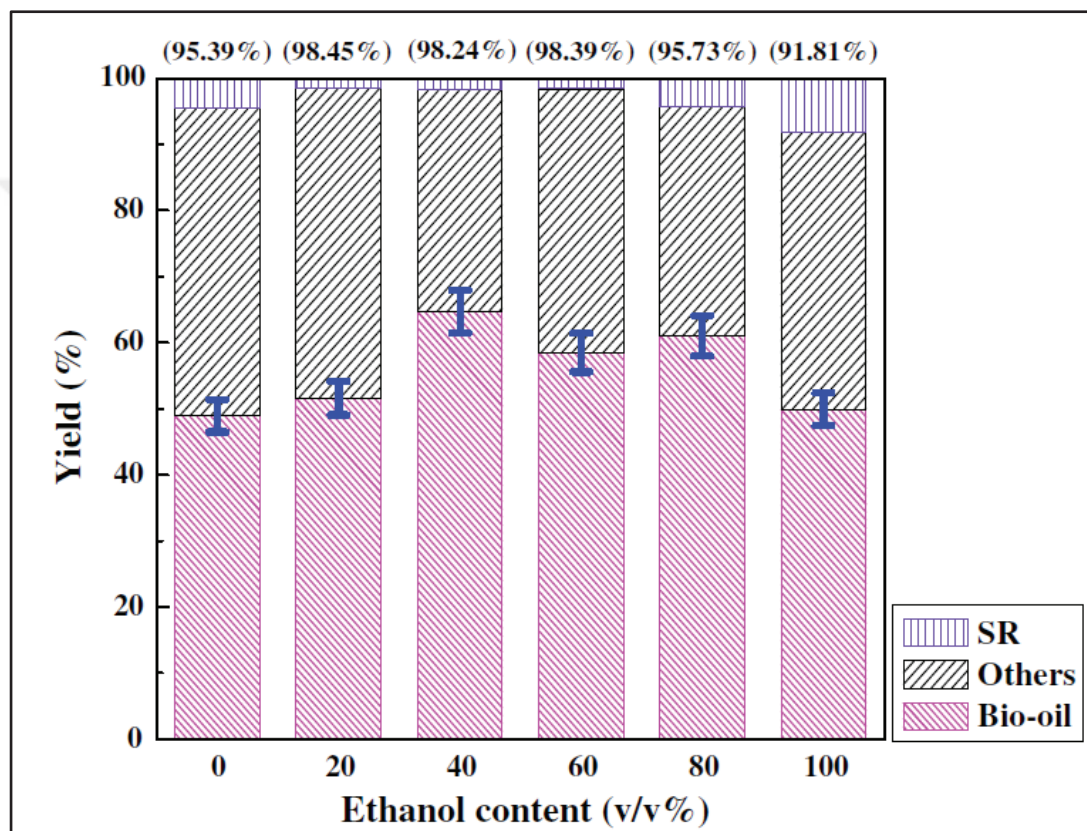


Figure 2.7. Effect of ethanol content on the bio-oil yield, solid residue and other (Source: Yu et al. 2012)

Effects of temperature, solvent/biomass ratio and reaction time on product yields in sub-and supercritical acetone were studied.¹⁹ Liquefaction experiments were carried out in temperature range (170-350 °C). Low conversion and bio-oil yield were obtained in sub critical acetone ($T < 235$ °C) region. Best bio-oil yield was observed at 290 °C as 60.1 % wt Figure 2.8. Above this temperature bio-oil yield started to decrease as a result of polymerization of intermediates high molecular compounds and it is possible that high temperatures tend to produce light end liquid products more volatile than acetone. Gas amount did not affect by temperature.

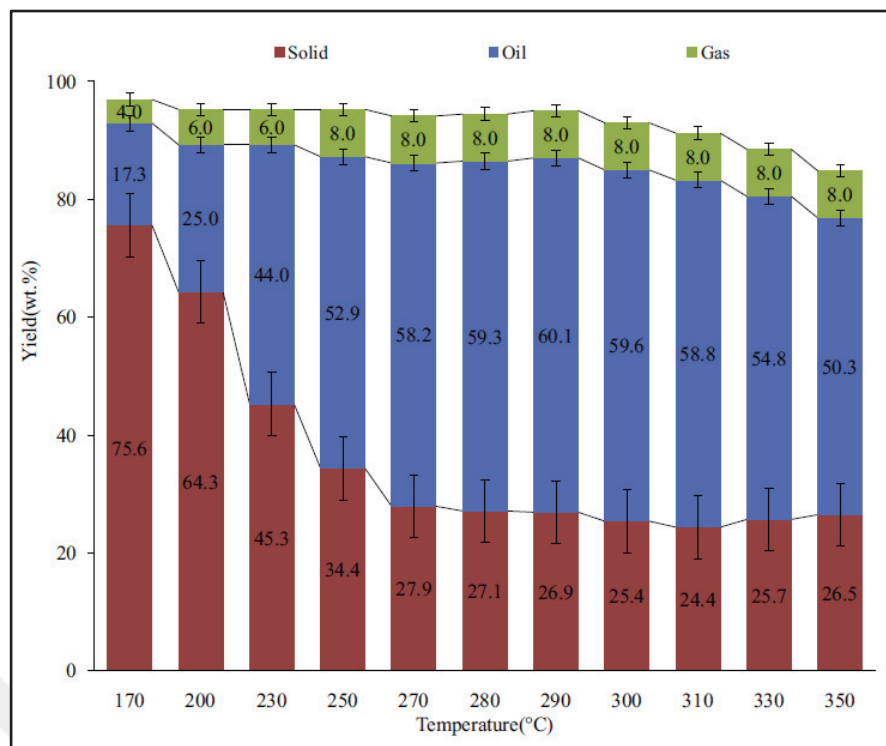


Figure 2.8. Effect of temperature on the yields of product fractions
(Source: Jin et al. 2014)

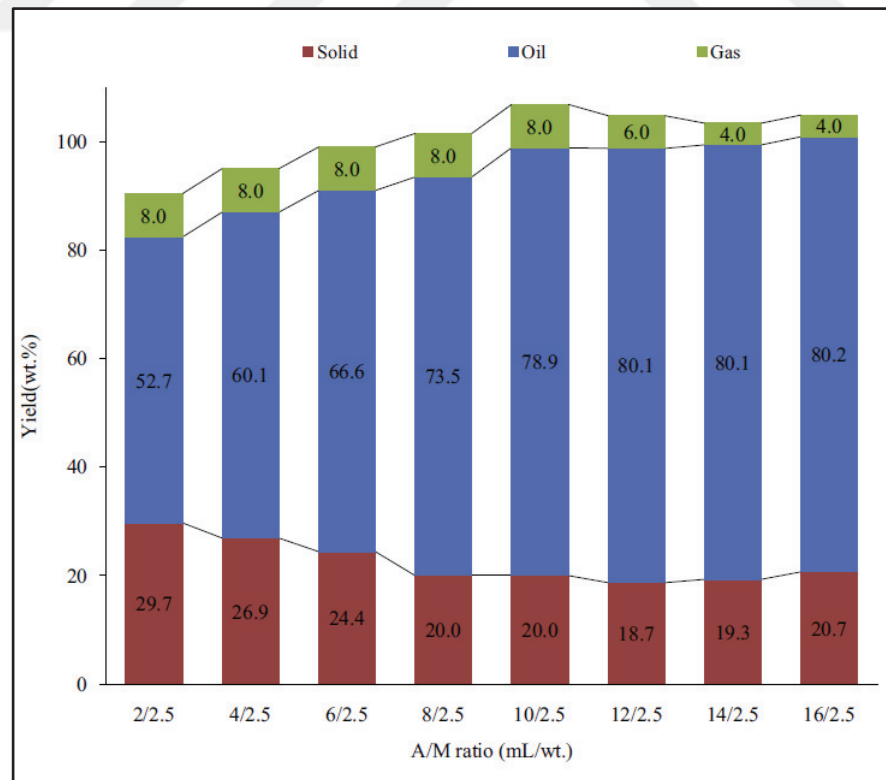


Figure 2.9. Effect of A/M ratio on the yields of product fractions
(Source: Jin et al. 2014)

Time is another parameter that affects the bio-oil yield Figure 2.10. The lowest and highest bio-oil yield were obtained at a reaction time of 5 min and 60 min as 63.7 and 78.9 wt%, respectively. After the reaction time of 60 min to 120 min slight decrement in bio-oil yield. This can be the result of possible secondary and tertiary reactions of the mixture. In other words, it can be simply said that saturation point of the reaction time was 60 min. According to GC-MS results, all process parameters have remarkable effect on product distribution.

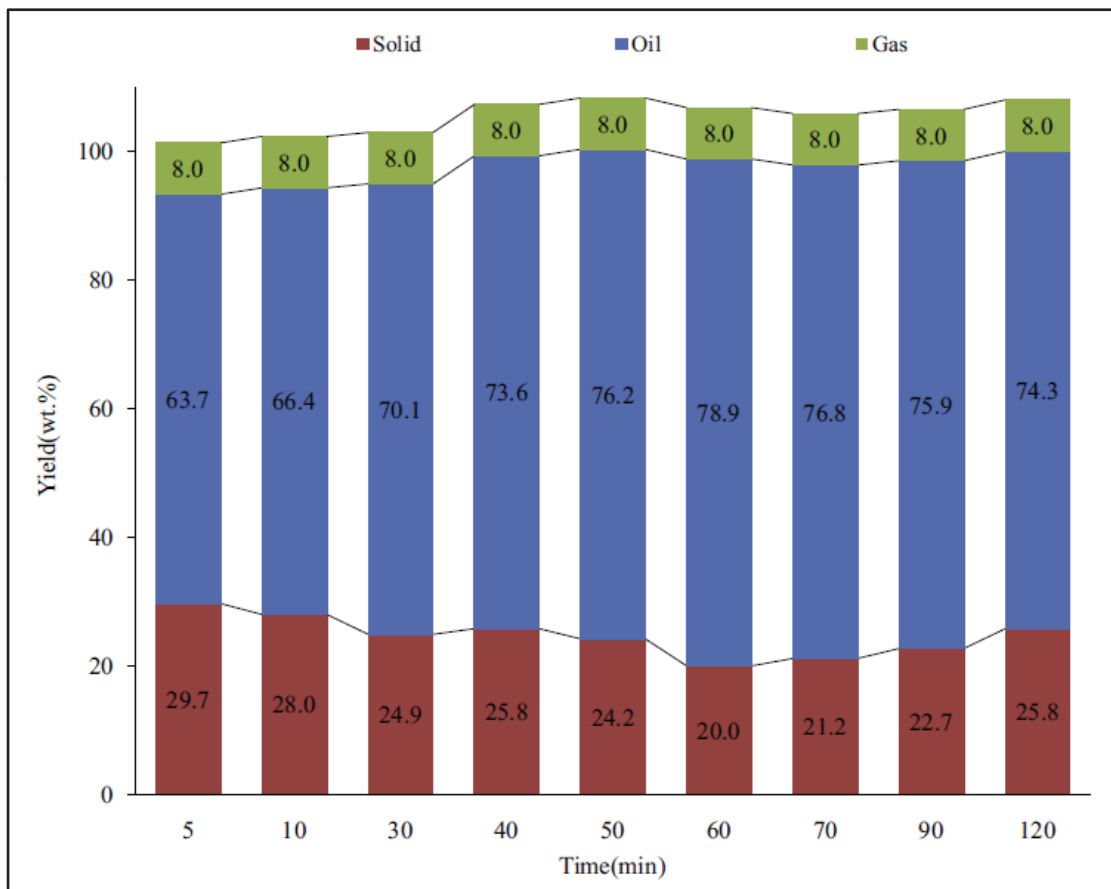


Figure 2.10. Effect of time on the yields of product fractions
(Source: Jin et al. 2014)

CHAPTER 3

MATERIALS AND METHODS

3.1. Chemicals and Material

Hazelnut shell (HNS) was supplied from Fiskobirlik A.Ş located in Giresun, Turkey. Ethanol (ACS grade) and acetone (ACS grade) were purchased from Merck. All chemicals that used in the structural analysis are listed Table 3.1.

Table 3.1. Chemicals used in Structural Analysis

Chemical Name	Manufacturer
Sodium lauryl sulfate	Merck
Ethylenediaminetetraacetic acid disodium salt dihydrate	Fluka
Disodium hydrogen phosphate	Sigma
Disodium tetraborate	Merck
Ethylene glycol monomethyl ether	Merck
Cetyl Trimethylammonium Bromide	Sigma
Sulfuric Acid	Merck

3.2. Experimental Setup

Experiments were carried out in a batch reactor (Parr 5500 Series, USA) made of SS-316 with a 300 mL of total volume equipped with a magnetic stirrer as can be seen Figure 3.1. The maximum operating conditions of this compact batch reactor are 350 °C of temperature, 207 bars of pressure and 300 ml of reactor volume. This reactor is equipped with pressure gage, gas inlet and outlet valves, rupture disc, an internal stirrer, an internally fixed thermocouple. The reactor is heated by aluminium block equipped 1000 W heat coil. Also, reactor has a cooling system that utilizes anti-freeze as a coolant. The flowrate and temperature of the coolant liquid is regulable.

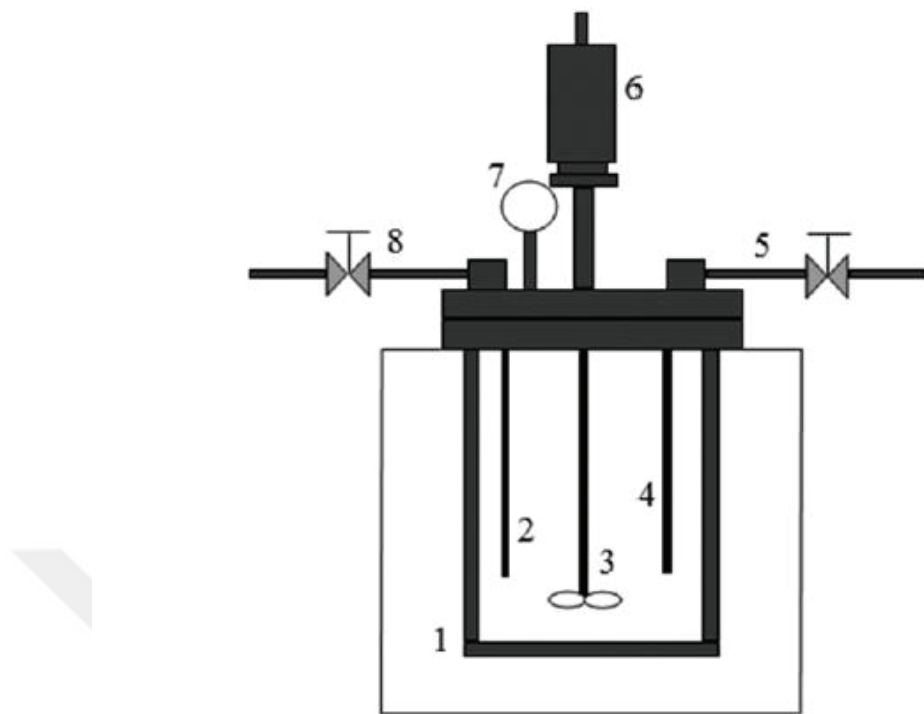


Figure 3.1. Thermochemical conversion reactor: (1) stainless steel vessel, (2) thermocouple, (3) stirring impeller, (4) gas inlet, (5) input nitrogen gas, (6) magnetically driven stirrer, (7) pressure gauge, (8) gas sample collector.

3.3. Experimental Procedure

Hazelnut shell (HNS) was supplied from Fiskobirlik A.Ş located in Giresun, Turkey. HNS was dried at 100 °C and was ground to particle size of 600 µm. 4 g (non-extracted and dry) HNS was loaded to reactor then reaction volume completed to 100 ml by addition of ethanol, acetone with different ratios. All nuts were tightened and safety collar worn. After that, the reaction medium was purged by using an inert gas (N₂) in order to remove oxygen inside the reactor. Then, the temperature was set to the desired reaction temperature with the heating rate of 7 °C/min. Stirring rate was 250 rpm during the experiments. At the end of the reaction, the heater was switched off and the system was cooled by two air fans with the cooling rate of 6 °C/min. The final sample was taken after the pressure becomes safe levels.

After the reaction, liquid and solid products were obtained. In order to separate liquid and solid part of the suspension was filtered through Whatman grade 307 filter paper under vacuum. The solid residue was dried 80 °C in an oven overnight. The solvent

was separated from the liquid part by using rotary evaporator under specific pressure and temperature according to the nature of the solvent. The bio-oil yield and solid conversion were calculated as using the following equations:

$$\text{Bio oil yield (\%)} = \frac{\text{Mass of bio oil}}{\text{Mass of initial hazelnut shell}} \times 100 \quad (3.1)$$

$$\text{Solid conversion (\%)} = \frac{\text{Mass of initial hazelnut shell} - \text{Mass of solid residue}}{\text{Mass of initial hazelnut shell}} \times 100 \quad (3.2)$$

3.4. Experimental Design

In order to determine the relationship between a variable and its effect on results, multiple experiments must be carried out by changing variables and follow the results. Also, obtained results can be analyzed by using statistical approaches. In this study, general full factorial experimental design was used to see effects of all variable combinations at the same. While generating factorial design and during statistical analysis, Minitab 17 software was used. Experimental design is tabulated in Table 3.2.

Table 3.2. Experimental Design of Hazelnut Shell Conversion

Experiment Code	Temperature (°C)	Time (min)	Ethanol/Acetone (v/v %)
1	220	30	0:100
2	220	30	25:75
3	220	30	50:50
4	220	30	75:25
5	220	30	100:0
6	220	60	0:100
7	220	60	25:75
8	220	60	50:50
9	220	60	50:50
10	220	60	75:25
11	220	60	100:0
12	220	90	0:100
13	220	90	25:75
14	220	90	50:50
15	220	90	75:25
			100:0

cont on the next page

Table 3.2 (cont)

Experiment Code	Temperature (°C)	Time (min)	Ethanol/Acetone (v/v %)
16	260	30	0:100
17	260	30	25:75
18	260	30	50:50
19	260	30	75:25
20	260	30	100:0
21	260	60	0:100
22	260	60	25:75
23	260	60	50:50
24	260	60	75:25
25	260	60	100:0
26	260	90	0:100
27	260	90	25:75
28	260	90	50: 50
29	260	90	75:25
29	260	90	75:25
30	260	90	100:0
31	300	30	0:100
32	300	30	25:75
33	300	30	50:50
34	300	30	75:25
35	300	30	100:0
36	300	60	0:100
37	300	60	25:75
38	300	60	50:50
39	300	60	75:25
40	300	60	100:0
41	300	90	0:100
42	300	90	25:75
43	300	90	50:50
44	300	90	75:25
45	300	90	100:0

3.5. Structural Carbohydrate Analysis

It is important to know composition of hazelnut shell to comment the results. In order to determine structural carbohydrate composition (cellulose, hemicellulose, lignin) in hazelnut shell, Van Soest method was used. Van Soest method includes separation of less digestible wall (cellulose, hemicellulose, lignin) and mostly digestible (starch, sugars) wall. The composition of hazelnut shell was given in Table 3.3. Van Soest has four stages. These are extraction, NDF (Neutral Detergent Fiber), ADF (Acid Detergent Fiber), ADL (Acid Detergent Lignin) analysis.

Table 3.3. Hazelnut Shell Composition

Structural Analysis (wt.%)	
Cellulose	36.02
Hemicellulose	12.66
Lignin	40.14
Extractives	7.86
Proximate Analysis (wt.%)	
Moisture	8.93
Ash	1.48
Protein	3.11

3.5.1. Extraction

Before the structural analysis, biomass must be separated from the extractives. Biomass initially were extracted via water for 2 hours. Then, biomass was extracted with the benzene: ethanol (2:1) mixture for 4 hours. In the final extraction stage, biomass was extracted with pure ethanol for 4 hours. Extractive free biomass was dried in an oven overnight.

3.5.2. NDF (Neutral Detergent Fiber) Analysis

This analysis provides to separate cell content from cell wall. Extracted dry biomass was boiled with NDF solution for 1 hour. After boiling, mixture was filtered through constant weight gooch crucible (G_1). Filtrated solid particles was washed with hot water three times to remove NDF solution and NDF soluble materials. Last washing was done by using 0.1 N HCl. After last washing, a beaker was filled with 0.1 HCl until 2/3 of the gooch crucible and was waited for 30 minutes. Gooch crucible was dried at 105 °C and weighted (G_2). From the G_2-G_1 difference (equation 3.3), NDF content was found. However, this part includes NDF ash. Dried gooch crucible was burned at 550 °C to determine NDF ash for 3 hours. NDF ash was determined by G_3-G_1 difference.

NDF solution contains; Sodium lauryl sulfate, Ethylenediaminetetraacetic acid disodium salt dihydrate, Disodium tetraborate, Disodium hydrogen phosphate, Ethylene glycol monomethyl ether.

$$\text{NDF \%} = 100 \times \left\{ \frac{G_2 - G_1}{\text{Sample weight}} \right\} \quad (3.3)$$

3.5.3. ADF (Acid Detergent Fiber) Analysis

This analysis provides to separate hemicellulose from the matrix. Dried biomass was boiled with ADF solution for an hour. Then, solution and biomass mixture were filtered through constant weigh gooch crucible (G₄). After filtration, solid particles were washed with deionized water three times, two times with pure acetone and dried at 105 °C. After drying, gooch crucible with biomass was weighted (G₅). ADF amount was found by using equation 3.4. ADF solution contains; Cetyl Trimethylammonium Bromide and 1 N H₂SO₄.

$$\text{ADF \%} = 100 \times \left\{ \frac{G_5 - G_4}{\text{Sample weight}} \right\} \quad (3.4)$$

3.5.4. ADL (Acid Detergent Lignin) Analysis

This analysis provides to determine lignin content in biomass. This analysis was a following step of ADF. Including ADF (G5) Gooch crucible was placed in a beaker that filled with 72% H₂SO₄. Biomass and acid solution were mixed to prevent agglomeration. After 3 hours, gooch crucible was washed with hot deionized water three times in order to remove sulfuric acid from the remaining solid. Then, gooch crucible was dried at 105 °C and weighted (G6). Cellulose percent was calculated by using equation 3.5.

$$\text{Cellulose \%} = 100 \times \left\{ \frac{G_5 - G_6}{\text{Sample weight}} \right\} \quad (3.5)$$

Gooch crucible was burned at 550 °C for 3 hours to find acid insoluble lignin. After burning crucible was weighted (G7). ADL was calculated by equation 3.6.

$$\text{Lignin \%} = 100 \times \left\{ \frac{G_6 - G_7}{\text{Sample weight}} \right\} \quad (3.6)$$

Hemicellulose amount in the hazelnut shell waste was calculated by using equation 3.7.

$$\text{Hemicellulose \%} = \text{ash-free NDF} - \text{ash-free ADF} \quad (3.7)$$

3.6. Product Analysis

After the reaction, liquid and solid products were separated in order to analysis. Liquid products were analyzed by GC-MS and solid residue were analyzed by using FTIR-ATR.

3.6.1. Liquid Product Analysis

Bio-oil samples were analyzed via gas chromatograph mass spectrometer (GC-MS, Agilent 6890 N/5973 N Network, USA). The carrier gas was He at a flowrate of 1 ml/min. HP-5MS column which is, (0.25 mm x 30 m x 0.25 μm) was used. Oven temperature was started from 40 °C. After that, holding 3 min, followed by 12 °C/min heating rate to 190 °C and hold 1 min. With the heating rate of 8 °C/min temperature was increased 190 to 300 °C. and hold 20 min. The injected volume was 1 μl with 10:1 split ratio.

3.6.2. Solid Product Analysis

Functional groups in bio-oil were examined in the wave number range of 4000-650 cm^{-1} by using Fourier Transform Infrared Spectrometry that equipped with attenuated total reflectance (ATR-FTIR) (Perkin Elmer-Spectra Two, USA).

CHAPTER 4

RESULTS AND DISCUSSION

4.1. Effect of Temperature

To investigate the effect of temperature on the conversion of waste hazelnut shell and bio-oil yield, experiments were carried out with varying temperatures such as 220 °C, 260 °C and 300 °C. The results obtained from the thermochemical liquefaction of waste hazelnut shell, including conversion and bio-oil yield are given in Table 4.1.

Table 4.1. Experimental results of hazelnut shell liquefaction at three different temperatures

Time (min)	EtOH:Ac (v:v)	at 220 °C		at 260 °C		at 300 °C	
		Conversion (wt.%)	Oil Yield (wt.%)	Conversion (wt.%)	Oil Yield (wt.%)	Conversion (wt.%)	Oil Yield (wt.%)
30	0:100	24.37	11.96	34.77	16.68	52.04	30.33
30	25:75	24.29	13.57	34.94	17.84	54.19	31.60
30	50:50	31.39	15.36	34.45	19.64	57.43	34.36
30	75:25	25.67	13.99	36.84	18.35	54.21	28.49
30	100:0	29.95	15.41	40.90	15.07	57.62	30.62
60	0:100	24.69	10.15	40.01	18.55	54.26	29.72
60	25:75	26.94	12.21	41.72	19.35	56.72	29.88
60	50:50	27.25	16.70	39.65	20.50	58.58	36.65
60	75:25	29.61	15.00	42.66	18.73	60.31	34.77
60	100:0	30.40	14.93	42.13	15.42	62.94	31.24
90	0:100	27.34	15.44	41.02	18.38	55.90	37.88
90	25:75	27.99	15.69	43.24	21.20	58.24	39.41
90	50:50	27.12	17.52	41.90	24.03	62.48	44.23
90	75:25	28.68	16.17	42.89	17.39	61.81	36.55
90	100:0	33.92	16.20	42.94	15.70	64.28	31.60

As it can be seen in Figure 4.1, Figure 4.2, and Figure 4.3, for the whole range of investigated temperatures, the conversion of waste hazelnut shell increased with increasing reaction temperature with respect to each solvent ratio (except 50/50 mixture of EtOH/Ac – v/v) and reaction time. It is distinguishable from Table 4.1 that, the highest hazelnut shell conversion was achieved in 300 °C by using pure ethanol solvent (100/0 –

v/v) for 90 min reaction time as around 64%, and the lowest was found in 220 °C by using pure acetone solvent (0/100 – v/v) for 30 min reaction time as around 24%.

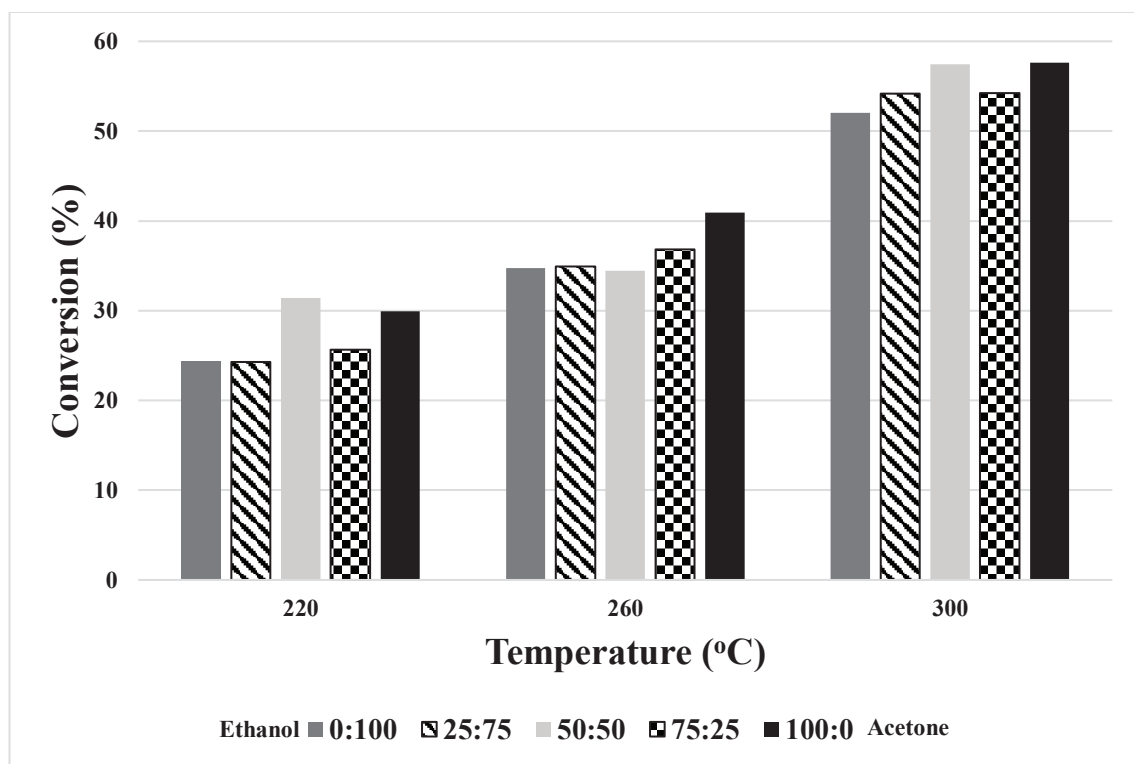


Figure 4.1. Temperature and solvent effects for hazelnut shell conversion for 30 min reaction time

Hazelnut shell like other biomasses consists of cellulose, hemicellulose and lignin structures, extractives and the structural analysis results, which was given in Table 3.3, show that cellulose, hemicellulose and lignin content of the hazelnut shell are 35.72%, 12.86%, 39.54% and 7.86%, respectively. Individual biomass constituents' (cellulose, hemicellulose and lignin) behavior in subsupercritical fluids gives us better insight about what is going on here. According to Brand and Kim, almost all of the hemicellulose is reached complete conversion at 265 °C, and cellulose has only 11.6% conversion at that temperature, individually.³⁰ Therefore, from this point of view it can be said that, at 220 °C nearly the whole degradation of hazelnut shell occurs mainly by hemicellulose and by little amount of cellulose. Because, when compared to cellulose and lignin, decomposition of hemicellulose at lower temperatures is easier than cellulose and lignin due to its amorphous structure.⁸ On the other hand, bio-oil yield at 220 °C is averagely around 14%, which is very low as expected. It is also consistent with the literature data due to Brand and Kim.

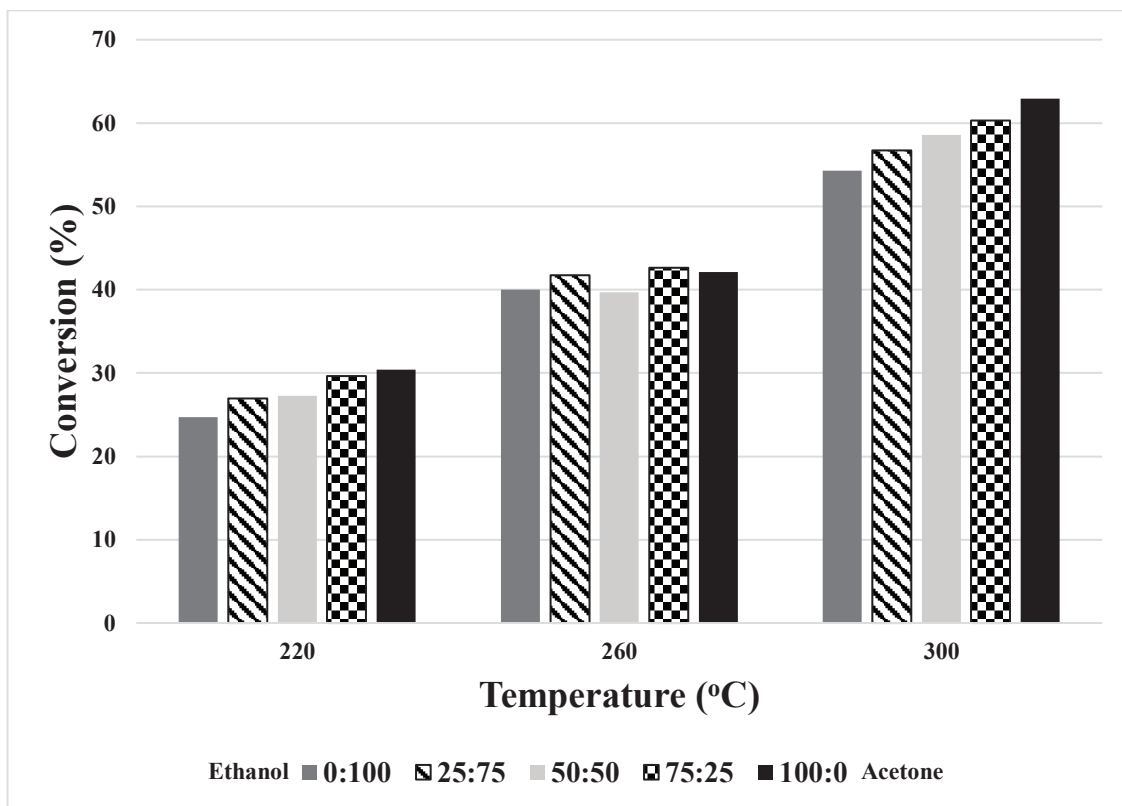


Figure 4.2. Temperature and solvent effects for hazelnut shell conversion for 60 min reaction time

Whereas, for other two temperatures (260 °C and 300 °C), experiments were carried out in supercritical region of both solvents. Therefore, it is plausible to think that, by passing into the supercritical region hazelnut shell conversion and bio-oil yield must be increased. The main reasons behind that are high diffusivity rates, low dielectric constant values and changing polarization in supercritical region.³²⁻³³ The results obtained from the supercritical ethanol liquefaction of hazelnut shell indicates that, by increasing temperature from 220 °C to 260 °C the average biomass conversion was increased from ca. 27% to 40%, while bio-oil yield was slightly increased from 14.7% to 18.5%. Conversion values seem to be consistent with the hypothesis, but there is a slight increment in bio-oil yield. However, this trend is still reasonable, because, as in the literature, mentioned Brand and Kim, feedstock cellulose gives only around 5% of bio-oil at 265 °C, while lignin has no data below 290 °C. Moreover, it's known that cellulose and lignin thermogravimetric analysis show similar weight loss until 350 °C, and decomposition of lignin is harder than cellulose.³⁰ For this reason, it is possible to think that very similar amount of bio-oil yield comes from lignin. These explains why there is a slight increment on bio-oil yield with respect to 220 °C.

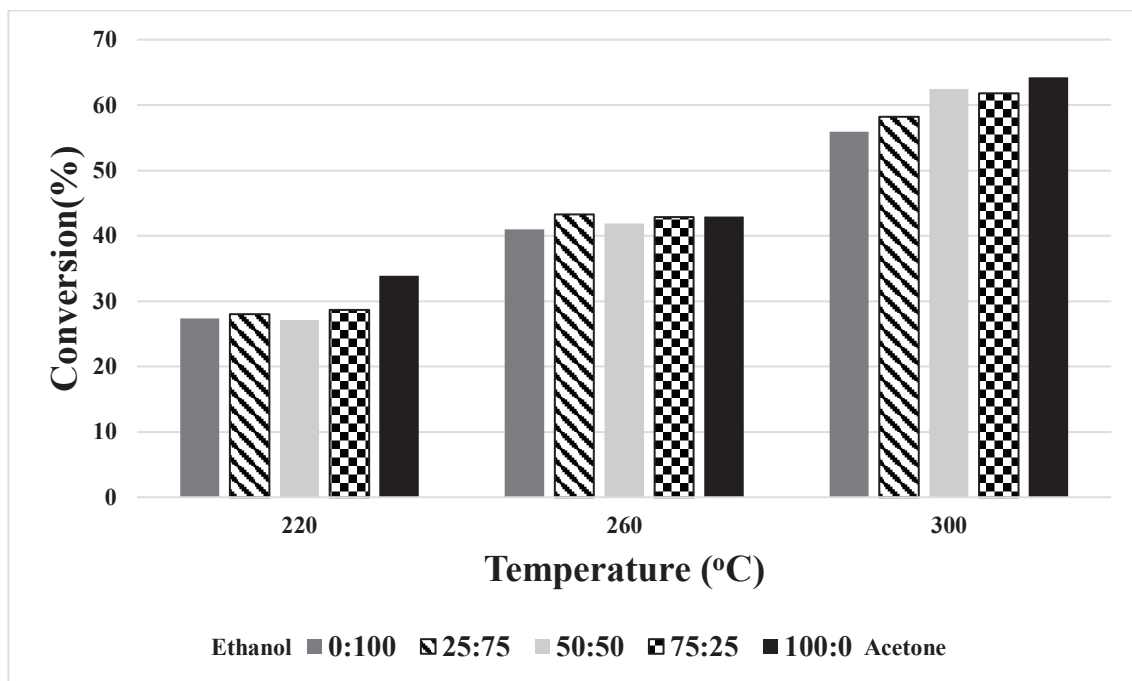


Figure 4.3. Temperature and solvent effects for hazelnut shell conversion for 90 min reaction time

By increasing the temperature from 260 °C to 300 °C, resulted with the increment of average hazelnut conversion from 40% to 58.1%, and almost doubling of bio-oil yield from 18.5% to 33.8%. Even if it's known biomass conversion and bio-oil yield strongly depends on biomass type and solvent type, the results obtained in this work consistent with some of the works in literature.^{8, 12, 14} Both cellulose and lignin above 250 °C decomposes by depolymerization reactions.³⁰ According to Table 4.1, it's not surprising there is a huge increment on bio-oil yield between 260 °C and 300 °C. In addition to that, the increment amount of biomass conversion between 260 °C and 300 °C is more than difference between 220 °C and 260 °C.

In summary, effect of temperature can be simply concluded as following sentences: at low temperatures, biomass decomposed and depolymerized to lighter molecule fragments at the beginning of liquefaction process. After that, unstable intermediates reacted with each other or ions/radicals of the solvents and rearranged through condensation and then followed by cyclization and polymerization that leads to new compounds. Temperature, here, is directly proportional to the defragmentation of the polymers. The higher the temperature of the reaction, the easier the fragmentation and combination of the polymers into bio-oil phase. By increasing the temperature more, forming of gaseous species will be enhanced, which is not in the scope of this study.

4.2. Effect of Solvents and Their Ratio

The experimental results of sub/supercritical ethanol and sub/supercritical acetone and their mixtures are given for solid conversion between Figure 4.1, Figure 4.2, Figure 4.3 and for bio-oil yield between Figure 4.4, Figure 4.5 and Figure 4.6. Different solvent ratios (EtOH/Ac - v/v): 0/100, 25/75, 50/50, 75/25, 100/0) were investigated for the solid conversion and bio-oil yield of hazelnut shell. At the temperature of 220 °C, bio-oil yield for pure ethanol is found slightly higher than pure acetone, whereas for biomass conversion ethanol gave more solid conversion than acetone for any temperature and time. This is probable because while approaching to near critical conditions, the density and dielectric constant decreases which leads to reducing interaction between hazelnut shell particles and solvent.³²⁻³³ As a result, liquid products yield will be less than the supercritical region. Since pure acetone has lower critical temperature (235 °C) than pure ethanol (241 °C), encountering with this behavior at 220 °C is likely. When we compare pure solvents (acetone and ethanol) with their mixtures (EtOH/Ac - v/v: 25/75, 50/50, 75/25), we can say there is no trend for conversion of biomass in mixture processes. On the other hand, it can be said that, there is a slight improvement on bio-oil yield by using solvent mixtures in experiments.

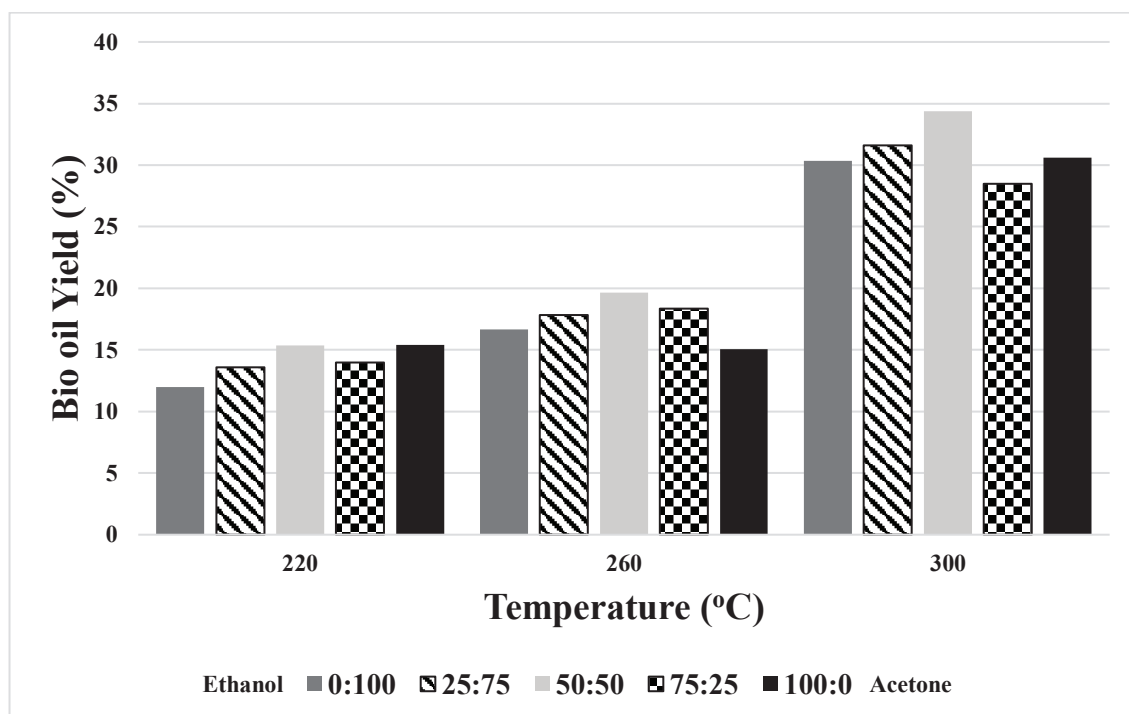


Figure 4.4. Temperature and solvent effects for bio-oil yield for 30 min reaction time

Based on the results presented in Figure 4.4, Figure 4.5 by increasing temperature from 220 °C to 260 °C, the experiments conducted with pure acetone caught the bio-oil yield of pure ethanol processes. And, also as mentioned in part 4.1, conversion increases by increasing temperature. When temperature is increased at some point it will be sufficiently high to break the solid biomass bonds and depolymerization occurs.²⁰ In solvents' aspect, when high temperature and pressure were applied on a polar protic solvent, which includes hydrogen bonding (pure ethanol), the hydrogen bonds in the cellulose and hemicellulose start to break down. Because of the glycosidic bonds of hemicellulose and cellulose are polar, and by the help of a polar protic solvent in sub/supercritical region they depolymerize very fast. Also, since ethanol has a big advantage which is hydrogen-bond donating, presence of ethanol as a solvent in thermochemical liquefaction processes stabilize the free radicals and help to obtain higher biomass conversion.³⁴ Acetone, on the other hand, is a dipolar aprotic solvent and does not include hydrogen bond to stabilize the reaction medium which leads to slightly lower biomass conversion as a result with respect to ethanol.

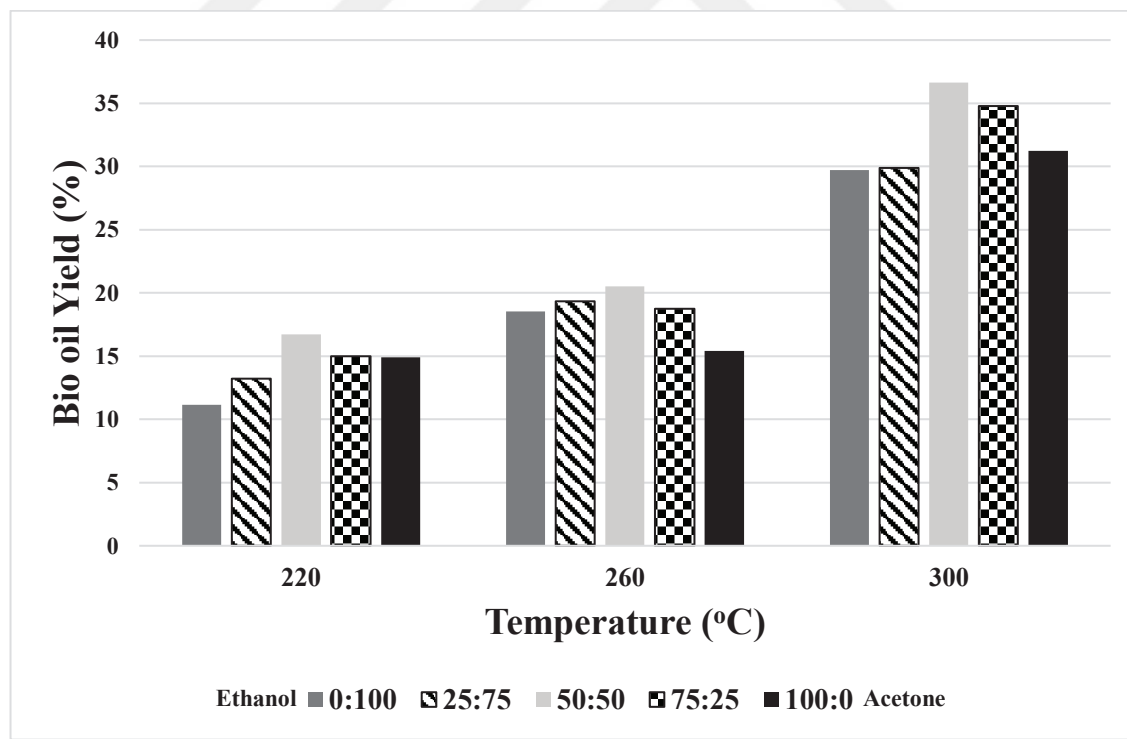


Figure 4.5. Temperature and solvent effects for bio-oil yield for 60 min reaction time

As it was mentioned in previous part, highest conversion and bio-oil yield of hazelnut shell was observed at 300 °C. Ethanol shows higher solid conversion for all of

three different time (30 min, 60 min, 90 min) compared to acetone and their mixtures. The reason behind that is the same as explained in the case of 260 °C. Nevertheless, by examining the bio-oil yield it can be seen that the highest bio-oil yield belongs to equal amount of solvent mixture (EtOH/Ac - v/v: 50:50). Also, it is apparent that bio-oil yield of the experiments conducted with pure acetone passes (max 37.88%) the pure ethanol processes (max 31.6%). First, it can be surprising for acetone to give more bio-oil yield with increasing temperature compared to ethanol. However, this is probable because of three characteristic of acetone solvent. It has lower critical pressure at 300 °C (8.6 MPa) rather than critical pressure of ethanol at 300 °C (11.2 MPa), aprotic solvent (no hydrogen bond donation) and less polar than ethanol.⁸ At high temperatures and pressures, solubility of solid strongly depends on the solvent pressure or, more appropriately, solvent density. If the pressure (or density) of the solvent is higher, the solubility of solid becomes lower. That means, repulsive forces between solvent and solute becomes dominant with respect to attractive forces between them.³³ Polarity of the acetone, on the other hand, is almost half of the ethanol, even if they have very similar critical temperature, density and dielectric constant values. That's the reason why ethanol is more efficient to solve polar compounds whereas acetone is more efficient for less polar compounds. Moreover, acetone is not a hydrogen donor solvent and does not show a stabilization effect as a solvent. If we combine them all, it is reasonable to have higher bio-oil yield in pure acetone processes at 300 °C, especially for 90 min rather than pure ethanol processes.

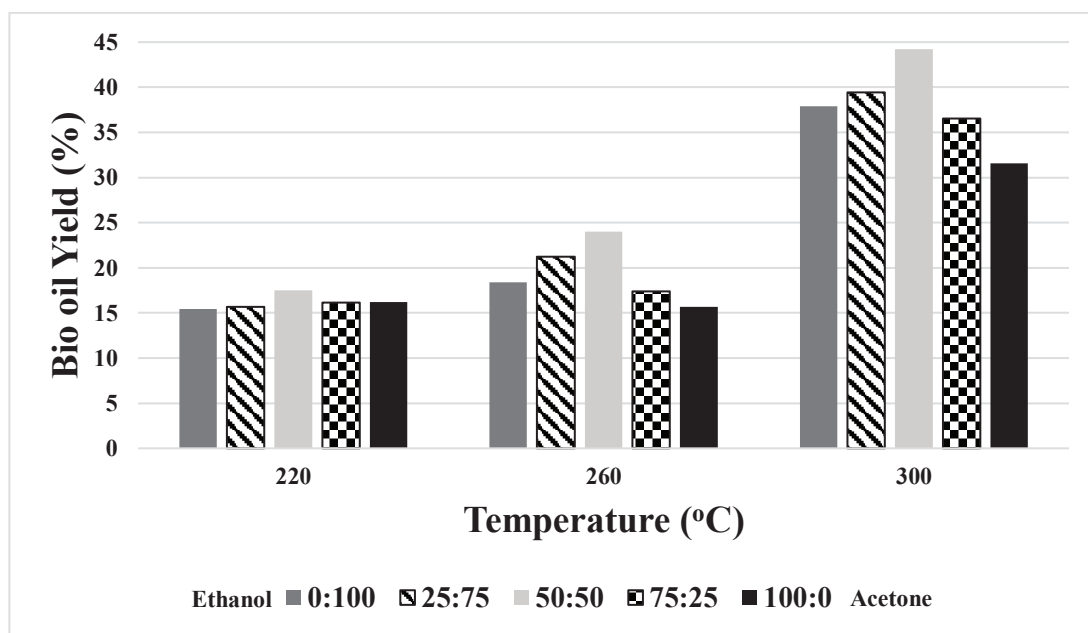


Figure 4.6. Temperature and solvent effect for bio-oil yield for 90 min reaction time

However, in the case of total extraction it is desirable to have high solid conversion and bio-oil yield. It is also acknowledged by increasing temperature, polarity, dielectric constant and hydrogen-bond donating abilities of the solvents decreases and behave like non-polar or close to non-polar solvents in supercritical region. Since the polarities of ethanol and acetone is different than each other, and it is known they show non-polar/less-polar behavior in supercritical region, maybe they were responsible for solving different organic compounds. Possibly while ethanol was decomposing a little bit polar compounds, acetone was in charge of degrading less or non-polar compounds. This hypothesis is also consistent with the experimental results showed in Figure 4.6. As mentioned above, highest bio-oil yield was found in 50/50 (v/v) ethanol/ acetone mixtures as 44.2%. It is obvious that acetone and ethanol showed synergetic effect on increasing bio-oil yield with increasing temperature and time. Even though it is clear from the results, their mixture effect in sub/supercritical region should also be explained thermodynamically to gain a better insight.

To explain these differences better, we have to consult the change of the polarity, dielectric constant and density values of these solvents in sub/supercritical region. How does dipole-moment change in sub/supercritical region and what is the effect of that change? Does acetone and ethanol form a complex in sub/supercritical region? What would be their thermodynamic behavior in sub/supercritical region? Unfortunately, to our best knowledge there is no thermodynamic study about above-mentioned properties except ethanol, which only covers until 250 °C.³² Therefore, there is a huge room for improvement in thermodynamic aspect for scientists to get a better insight.

4.3. Effect of Reaction Time

Degradation of hazelnut shell showed slight increments with increasing time for both biomass conversion and bio-oil yield for each temperature and solvent ratio as indicated between Table 4.2, Table 4.3 and Table 4.4. For experiments conducted at 220 °C, results showed similar behavior. Increasing time leads to slight increment of conversion and bio-oil yield within the error percentage for each solvent except 50/50 (v/v) mixture of acetone and ethanol for conversion. It shows opposite behavior compared to other solvents. Its value decreases from 31.4% (30 min) to 27.12% (90 min). This could be because of different effect of acetone and ethanol in subcritical region. There may be

some products occurred at 30th min and some of these products later can be repolymerized onto the solids at 90th min that stabilization effect of ethanol could not overcome. At 220 °C lowest solid conversion values were found for acetone solvent and highest for ethanol solvent for each time set. Mixtures hazelnut shell conversion values were dispersed between them.

Table 4.2. Change of biomass conversion and bio-oil yield with respect to time and solvent ratio at 220 °C

Solvent Ratio	Hazelnut Shell Conversion			Bio-Oil Yield		
	30 min	60 min	90 min	30 min	60 min	90 min
0:100	24.37	24.69	27.34	11.96	10.15	15.44
25:75	24.29	26.94	27.99	13.57	12.21	15.69
50:50	31.39	27.25	27.12	15.36	16.70	17.52
75:25	25.67	29.61	28.68	13.99	15.00	16.17
100:0	29.95	30.40	33.92	15.41	14.93	16.20

Table 4.3. Change of biomass conversion and bio-oil yield with respect to time and solvent ratio at 260 °C

Solvent Ratio	Hazelnut Shell Conversion			Bio-Oil Yield		
	30 min	60 min	90 min	30 min	60 min	90 min
0:100	34.77	40.01	41.02	16.68	18.55	18.38
25:75	34.94	41.72	43.24	17.84	19.35	21.20
50:50	34.45	39.65	41.90	19.64	20.50	24.03
75:25	36.84	42.66	42.89	18.35	18.73	17.39
100:0	40.90	42.13	42.94	15.07	15.42	15.70

The solid biomass conversion results obtained from the 260 °C demonstrates that increasing time is important only between 30 min and 60 min experiments. It can be said there is no difference between 60 min and 90 min applications. It is obvious from the Table 4.3, with increasing time there is no change in bio-oil yield for pure acetone, pure ethanol and 75/25 (EtOH/Ac - v/v) mixture solvents. On the other hand, by increasing time 50/50 and 25/75 (EtOH/Ac - v/v) mixtures shows an increment in bio-oil yield. Acetone seems to be more effective solvent during these temperatures and time range than ethanol. Highest values of bio-oil yield were observed for 260 °C and 90 min with

the solvents of 50/50 and 25/75 (EtOH/Ac - v/v) mixtures, as 24.03% and 21.20%, respectively.

Comparing the reaction time effect for each solvent for the experiments carried out at 300 °C shows that there is a slight increment on hazelnut shell conversion between each operation time. Increasing time allows to decomposition of polymeric constituents of biomass and let formed intermediate species enough time to react and shape new compounds or to stabilize. As mentioned above, polarity plays a big role here, since other properties of acetone and ethanol is similar to each other. Increasing the reaction time between 30 min and 60 min does not affect bio-oil yield that much. It can be seen from the Table 4.4, there is almost no change or too small change in bio-oil yield. However, when the operation time is increased to 90 min, except pure ethanol, there is more than 20% increment for bio-oil yield with respect to the experiments carried out at 260 °C. The highest bio-oil yield was observed for 50/50 (v/v) mixture as 44.2%. Pure acetone, 25/75 and 75/25 (EtOH/Ac - v/v) solvent mixtures gave very close bio-oil yields and pure ethanol remains to have the lowest bio-oil yield. Therefore, it can be said that acetone clearly increases the bio-oil yield of hazelnut shell and mixture of acetone and ethanol show synergistic effect to obtain higher bio-oil yield than pure solvents.

Table 4.4. Change of biomass conversion and bio-oil yield with respect to time and solvent ratio at 300 °C

Solvent Ratio	Hazelnut Shell Conversion			Bio-Oil Yield		
	30 min	60 min	90 min	30 min	60 min	90 min
0:100	52.04	54.26	55.90	30.33	29.72	37.88
25:75	54.19	56.72	58.24	31.60	29.88	39.41
50:50	57.43	58.58	62.48	34.36	36.65	44.23
75:25	54.21	60.31	61.81	28.49	34.77	36.55
100:0	57.62	62.94	64.28	30.62	31.24	31.60

4.4. Analysis of Variance (ANOVA)

Statistical analysis of time, temperature and ethanol/acetone ratio (v/v) were investigated on biomass conversion and bio oil yield to evaluate the significance of results by ANOVA via using MINITAB 17 software. Significance level was accepted as 95%

($p \leq 0.05$) Histograms and residual plots show the linear distributed data (Figure 4.7 and Figure 4.8). This confirms the model accuracy.

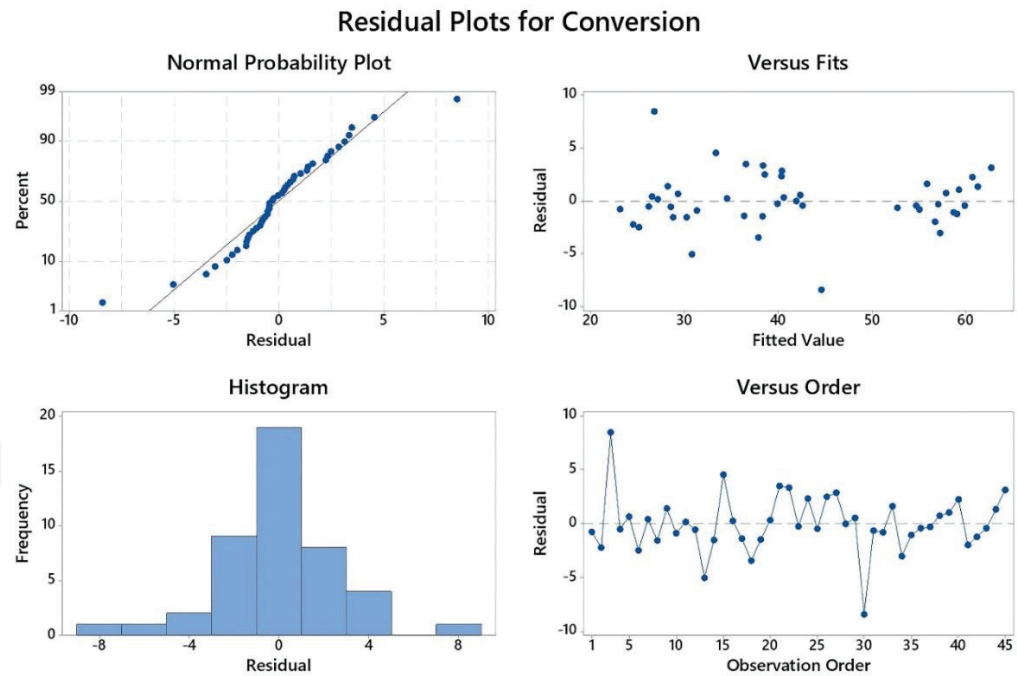


Figure 4.7. Histogram plots of conversion of hazelnut shell waste

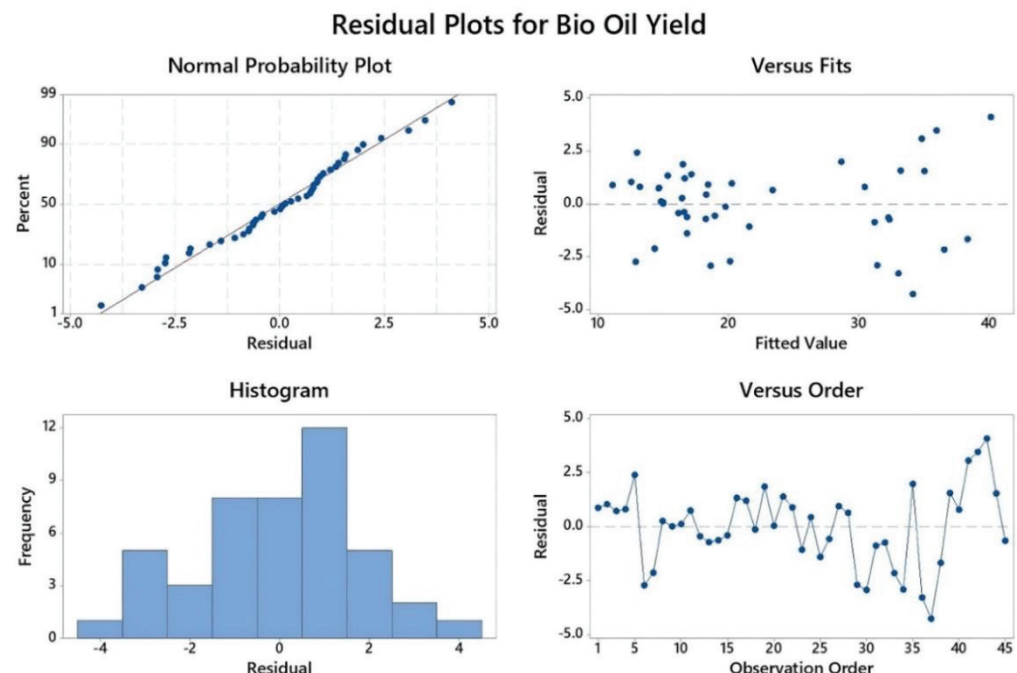


Figure 4.8. Histogram plots of bio oil yield from hazelnut shell waste

Table 4.5. Statistical analysis results of hazelnut shell conversion and bio oil yield (non-reduced model)

Source	DF	Adj SS	Adj MS	F-Value	p-Value
Model	17	3399.09	199.95	60.95	0.000
Linear	6	2970.75	495.12	150.93	0.000
Temperature	1	2745.64	2745.64	836.97	0.000
Time	1	97.63	97.63	29.76	0.000
Ratio	4	127.48	31.87	9.72	0.000
Square	2	348.55	174.28	53.13	0.000
Temperature - Time	1	336.40	336.40	102.55	0.000
Temperature - Time - Time	1	12.15	12.15	3.70	0.065
2-Way Interaction	9	79.79	8.87	2.70	0.022
Temperature-Time	1	27.68	27.68	8.44	0.007
Temperature-Ratio	4	33.05	8.26	2.52	0.065
Time-Ratio	4	19.07	4.77	1.45	0.244
Error	27	88.57	3.28		
Total	44	3487.66			

Table 4.5 shows ANOVA results of hazelnut shell conversion and bio- oil yield. While all individual parameters (temperature, time and ethanol/acetone ratio - v/v) affect the conversion and bio oil yield ($p \leq 0.05$), some 2-way interactions are not significant on conversion and bio oil yield like temperature-ratio and time-ratio because of their p-values are greater than 0.05. Table 4.6 describes reduced model of hazelnut shell conversion and bio- oil yield. After reduction of model p-values of all model terms are smaller than 0.05.

Table 4.6. Statistical analysis results of hazelnut shell conversion and bio oil yield (reduced model)

Source	DF	Adj SS	Adj MS	F-Value	p-Value
Model	8	3334.83	416.85	98.19	0.000
Linear	6	2970.75	495.12	116.62	0.000
Temperature	1	2745.64	2745.64	646.72	0.000
Time	1	97.63	97.63	23.00	0.000
Ratio	4	127.48	31.87	7.51	0.000
Square	1	336.40	336.40	79.24	0.000

Cont on the next page

Table 4.6 (cont)

Temperature-	1	336.40	336.40	79.24	0.000
Temperature					
2-Way Interaction	1	27.68	27.68	6.52	0.015
Temperature-Time	1	27.68	27.68	6.52	0.015
Error	36	140.69	4.25		
Total	44	3475.51			

Response surface plots for conversion and bio oil yield, when ethanol/acetone v/v% ratio holding constant, were shown in Figure 4.9 and Figure 4.10. Temperature and time have positive effect on hazelnut conversion and bio oil yield. While conversion is increasing from 25.78 to 62.48%, bio-oil yield is increased from 17.52 to 44.23% for 90 min, 300 °C and 50:50 ethanol/acetone (v/v) ratio.

The optimization results for hazelnut conversion and bio oil yield were given in Figure 4.11. Hazelnut shell waste conversion and bio oil yield were maximized as response. According to response optimization, optimum results for maximum conversion and maximum bio oil yield were found at 300 °C, 90 min and 50:50 ethanol/acetone (v/v) ratio, 59.86 and 40.12%, respectively. These results were calculated by considering r-squares values of model via minitab 17. Furthermore, model includes errors and uncertainties.

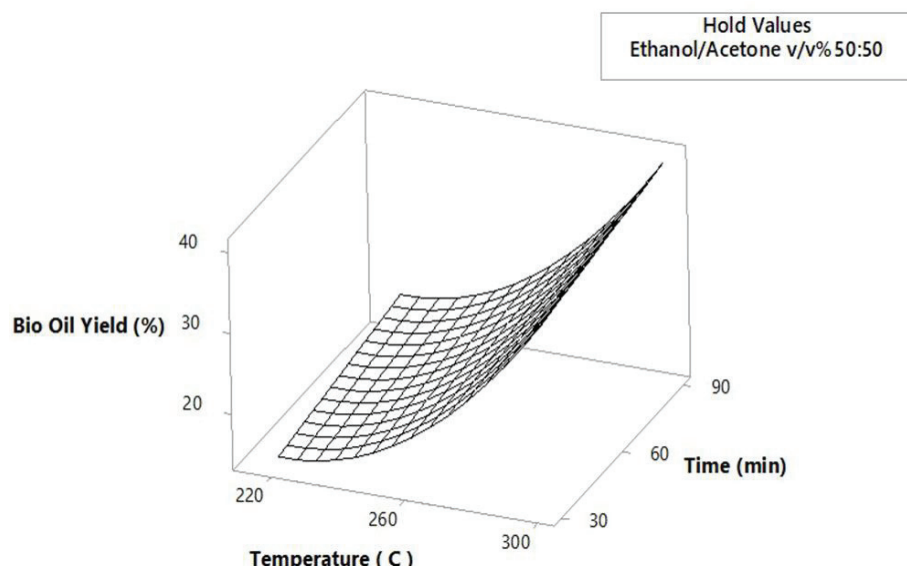


Figure 4.9. Response surface plot of Bio oil yield from hazelnut shell waste

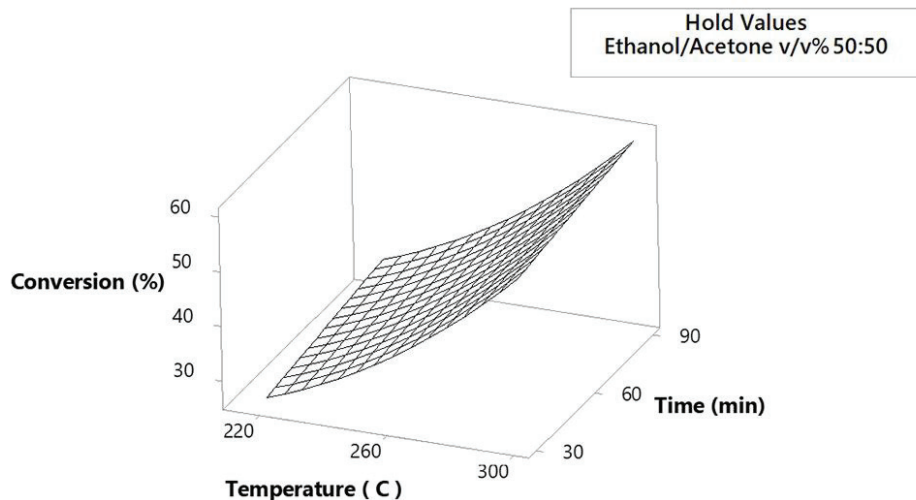


Figure 4.10. Response surface plot for the conversion of hazelnut shell waste

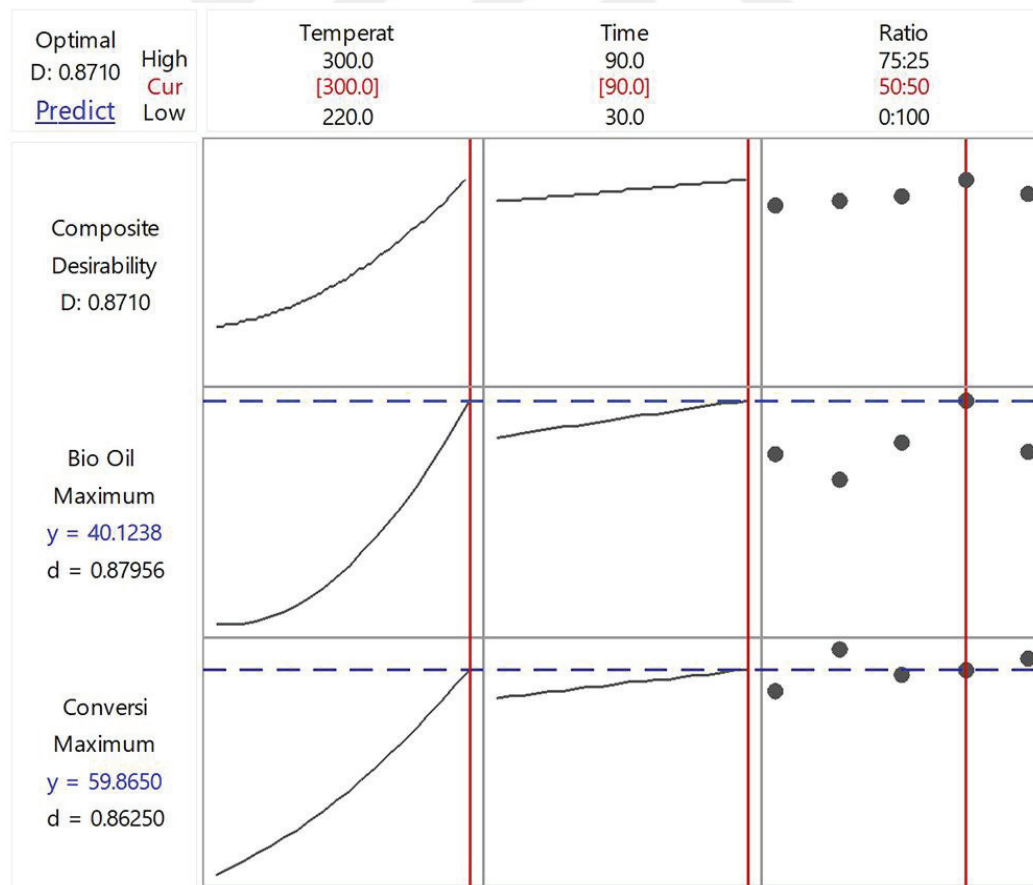


Figure 4.11. Optimum operating conversion for maximum conversion and maximum bio oil yield

4.5. GC-MS Analysis

The major chemical compounds formed in bio-oil products at 300 °C by using sub/supercritical ethanol, acetone and their mixtures (EtOH/Ac v/v): 25/75, 50/50 & 75/25) are characterized by GC-MS analysis and presented in Table A.1. As it can be seen from the table, according to their chemical functional groups 5 different major groups (e.g. acids, aldehydes & ketones, cyclic compounds, esters and phenolic compounds) constitute lots of the components in the table. More detailed analysis of chemical compounds in bio-oil can lead to understand better the reaction pathways occurred during sub/supercritical ethanol, acetone and their mixtures liquefaction. For this reason, thermodynamic behavior of the solvents and their mixtures must be studied first, and then from beginning with simple molecules (e.g. glucose, xylose) and following with their polymers (e.g. cellulose, hemicellulose) a detailed set of experiments must be done to have a better insight on reaction kinetics and mechanism.

Phenol is mainly generated by the degradation of low molecular weight lignin.³⁵ The lowest total phenolic content yield can be seen in the bio-oil products of 50/50 (v/v) mixture of ethanol and acetone. Previous studies mentioned that having no phenolic compound in the oil product is a sign of delignification operation.³⁶⁻³⁷ However, that is not the only sign of lignin presence. Aromatic compounds are also mainly degraded from lignin.³⁸ Since low amount of phenolic compounds still exist in bio-oil product, total delignification cannot be mentioned, but it can be said that, 50/50 (v/v) mixture of ethanol and acetone is a better delignifying solvent mixture than pure solvents and different mixture ratios.

Acetic acid and formic acid are fall into low molecular weight acid species and they tend to form as decomposition products of biomass during hydrothermal liquefaction. Forming of low molecular weight species during thermochemical liquefaction can cause thermal instability, high corrosiveness, and high tendency for polymerization.³⁹⁻⁴¹ Increment of pH values in the biocrude is a sign of acid formation during the operation. Hydrothermal liquefaction of a biomass type at 330 °C gave pH values of 4-4.5 can be given as an example.⁴² In another work that is carried out to decompose cellulose in subcritical water amount of acetic and formic acid increased from around 5.0% to 61.0% with an increase in residence time from 0.9 to 8.8s.⁴³ As listed in Table A.1, acetic acid and formic acid were not observed during GC-MS analysis of bio-

oil produced for any solvents. Some acids are found in bio-oil product, which are known as coming from decomposition of hemicellulose and cellulose. Only derivatives of them which are cyclohexyldiene acetic acid and 4-hydroxy-3-methoxy phenylacetylformic acid were found with increasing ethanol ratio but as very low amount. As an acid, mainly butanoic acid, butanedioic acid, tetradecanoic acid, propanoic acid, n-hexadecanoic acid and oleic acid themselves or derivatives were detected in GC-MS analysis instead of formic and acetic acid. Hence, it can be said the acidity of bio-oil products obtained by supercritical ethanol, acetone and their mixtures bio-oil product has much lower acidity than hydrothermal liquefaction.

Long chain ester formation is a unique feature of supercritical ethanol operations.³⁰ It can be seen from the Table A.1. There is no ester formation belongs to the experiments conducted in acetone medium except 9,12-octadecadienoic acid ethyl ester and 14-methyl pentadecanoic acid methyl ester. All other ester compounds were formed in the presence of ethanol. 2-hydroxy butanoic acid ethyl ester, 4-oxo-pentanoic acid ethyl ester, butanedioic acid diethyl ester, pentanedioic acid diethyl ester, 2'-hexyl 1,1'-bicyclopropyl-2-octanoic acid methyl ester, 4-hydroxy-3-methoxy benzoic acid ethyl ester, 14-methyl pentadecanoic acid methyl ester, hexadecanoic acid ethyl ester, linoleic acid ethyl ester, 10-octadecenoic acid methyl ester, 9,12-octadecadienoic acid ethyl ester, ethyl oleate, and octadecanoic acid ethyl ester were identified in gas chromatography analysis. Formation of lots of ester compounds in bio-oil product is a feature of supercritical ethanol that distinguishes it from other solvents. These products were not observed by using hydrothermal liquefaction processes.^{12, 43} Maybe glucose fragments were esterified in supercritical ethanol medium and produced these unique long-chain ester compounds. Also, it is worth mentioning here that natural triglycerides esterification in supercritical ethanol is a well-known area and leads to production of fatty acid methyl esters.⁴⁴⁻⁴⁶ In this study, by checking the Table A.1, it is obvious to see that the oleic acid (fatty acid) undergoes esterification reaction by interacting with increasing amount of alcohol and produces large amount of ethyl oleate (oleic acid ethyl ester). Formation of ester compounds leads to bio-oil to have low acidity, low corrosiveness, high molecular weight species and stability.³⁰

In overall, hazelnut shell liquefaction in supercritical ethanol, and its mixtures with acetone showed that ethyl oleate is the highest amount of compound found in each bio-oil product. On the other hand, acetone has the highest amount of oleic acid with respect to GC-MS analysis results. In supercritical ethanol liquefaction of hazelnut shell,

second and third major peaks are also belonging to ethyl esters, which are 9,12-octadecadienoic acid ethyl ester and hexadecanoic acid ethyl ester, respectively. Second and third major peaks of supercritical acetone liquefaction of hazelnut shell were found as 4-ethyl-2-methoxy phenol and 2-methoxy phenol, respectively. It is easy to perceive from the table, supercritical acetone and supercritical ethanol hazelnut shell liquefaction operations leads to different product distribution. Dielectric constant and density of ethanol and acetone is very close to each other, but critical pressure and polarity differs from each other and these features allow them to solve different compounds from the biomass and let intermediates follow different reaction pathways and different molecules collision. It has to be mentioned here also, by increasing temperature decreasing dielectric constant of both solvents and changing behavior of them from polar to non-polar solvents are the main reasons why high-molecular weight non-polar species bonds break and solve. In addition to these features, ethanol's hydrogen donor ability can be added, which is responsible for the esterification reactions of fatty acids in biomass that makes bio-oil product more stable [25, 26, 28]. It is distinguishable from the table that, solvent mixtures of ethanol and acetone (EtOH/Ac – v/v: 25/75, 50/50, 75/25), showed higher degradation than pure solvents, since there are more compounds for each solvent mixture. It is reasonable because in part 4.2 it was indicated as solvent mixtures bio-oil yield are higher than pure solvents bio-oil yield, especially 50/50 mixture separate from the other ones by having the highest bio-oil yield. Since ethanol and acetone are responsible to solve different polarity compounds and different reaction pathways, they are able to show synergetic effect to solve hazelnut shell better.

4.6. FT-IR Analysis

The functional groups of hazelnut shell were investigated by FTIR-ATR and the results are shown in Figure 4.12, Figure 4.13 and Figure 4.14. According to the literature⁴⁷⁻⁴⁸, peaks around 3316 cm^{-1} corresponds to the vibration of -OH groups. The peak of -OH band is broad because of overlapping and combination of aliphatic and aromatic O-H groups.⁴⁹ Hazelnut shell is composed of cellulose, hemicellulose and lignin. The bands at 2920 cm^{-1} , 2851 cm^{-1} and 1026 cm^{-1} belong to usual cellulose and hemicellulose structures that imply C-H bending of alkanes, saturated aliphatic C-H bending and beta-glycosidic bond, respectively.^{35, 50} The absorption at 1400 and 1600cm^{-1}

¹ shows the lignin (benzene ring) in the raw material.⁴⁹ In addition, peak at the 1605 cm⁻¹ refers to C=C aromatic stretching bond and peak 1742 shows C=O stretching in ketone, esters group. Peaks at 2920, 2851 and 1026 cm⁻¹ almost disappeared at 300 °C from the Figure 4.12. This is because of the degradation of hemicellulose and cellulose with the supercritical ethanol-acetone mixture. Furthermore, from the Figure 4.13 the signal at 2981 cm⁻¹ stretching C-H bond in alkyl groups is clear in 30 and 60 min. However, the same peak almost disappeared in 90 min. The absorption peaks at 1400 and 1600 cm⁻¹ did not disappear at all temperatures. It means that lignin does not completely decompose at these temperatures. Figure 4.14 represents that different ethanol/acetone (v/v) ratios do not show a difference at any peaks. It is concluded that solvents do not have the tendency to competition.

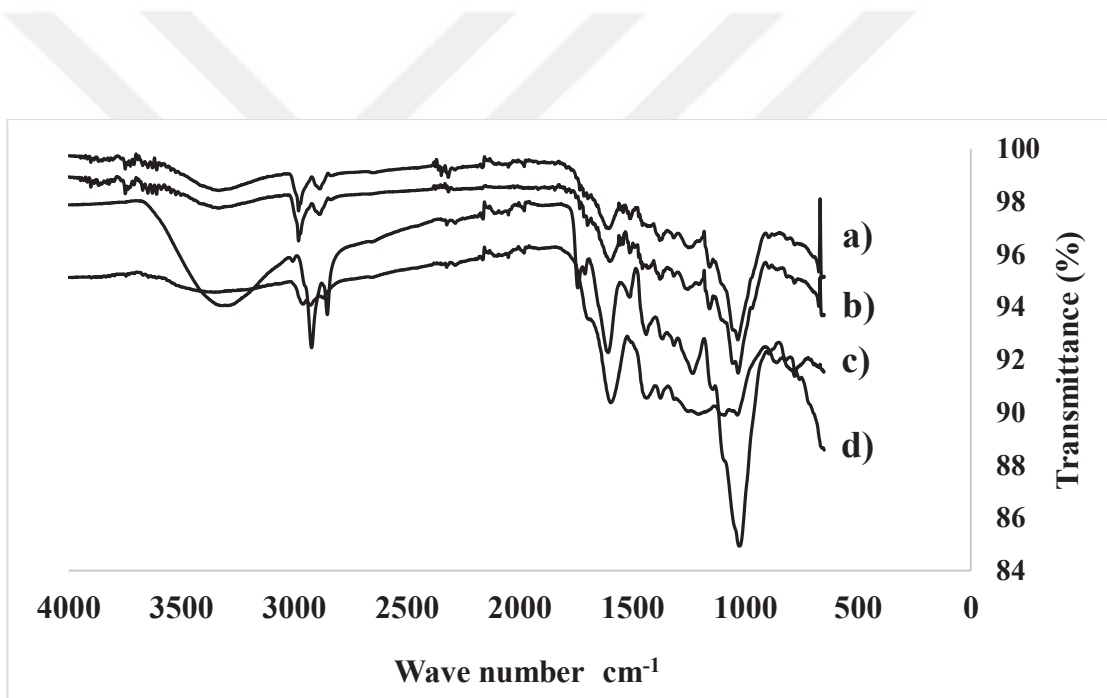


Figure 4.12. FT-IR spectrum of untreated and treated hazelnut shell samples at different temperatures a) 220 °C b) 260 °C c) Raw Material d) 300 °C

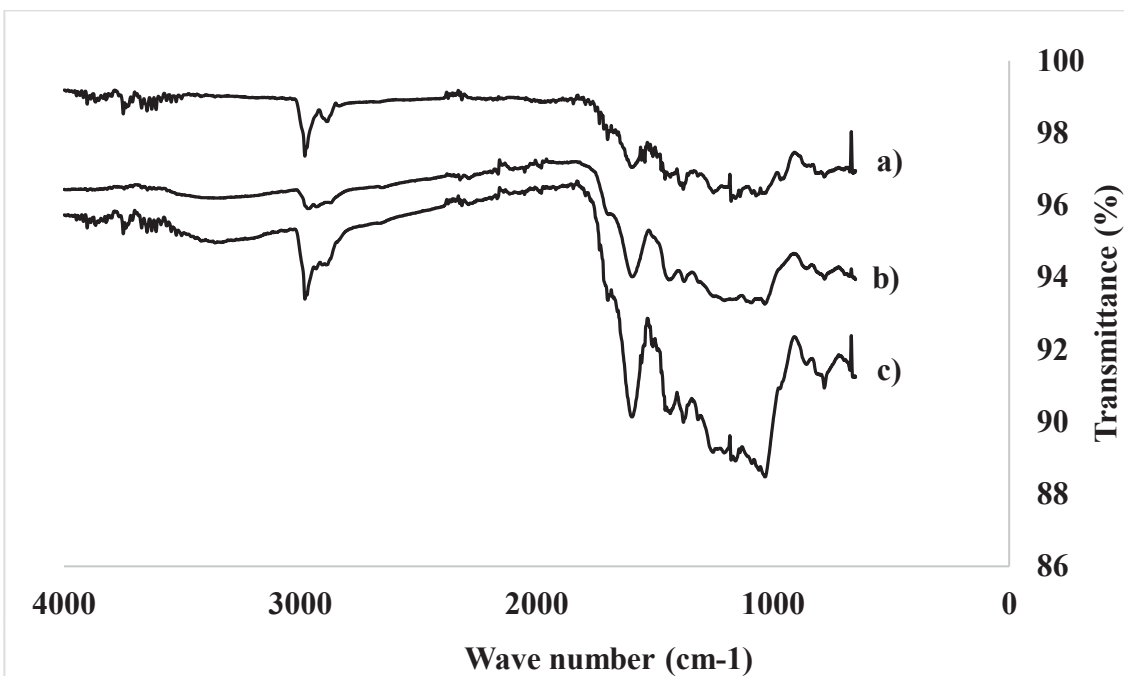


Figure 4.13. FT-IR spectrum of treated hazelnut shell samples at different reaction times at 300 °C a) 60 min, b) 90 min c) 30 min

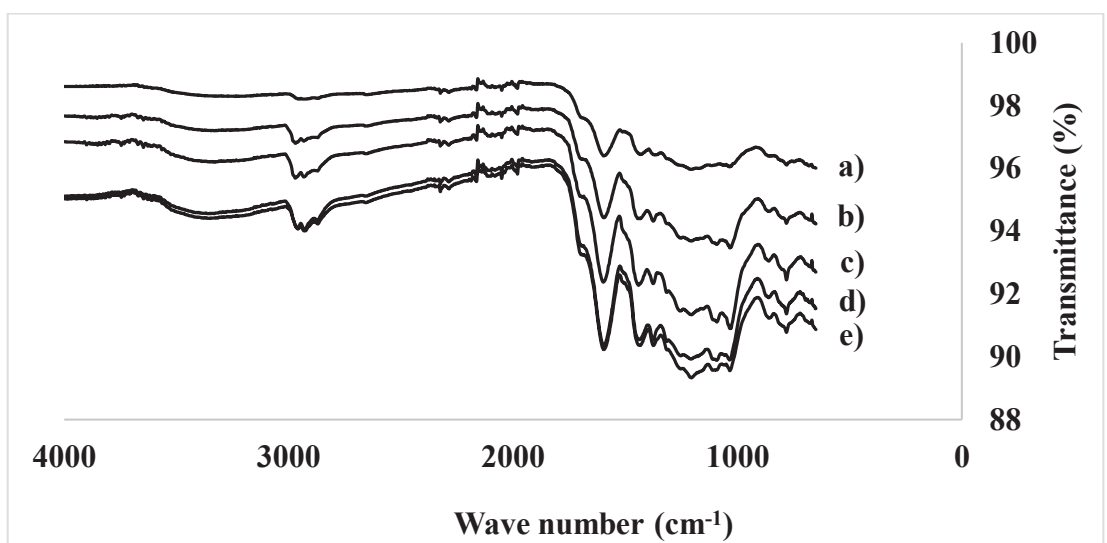


Figure 4.14. FT-IR spectrum of treated hazelnut shell samples with different ethanol/acetone (v/v) at 300 °C a) 0:100 b) 75:25 c) 100:0 d) 50:50 e) 25:75

CHAPTER 5

CONCLUSION

Reaction temperature, time and different ethanol/acetone (v/v) ratios were determined as the effective process parameters in achieving high conversion and bio-oil yield in thermochemical conversion of hazelnut shell. By increasing temperature, conversion and bio-oil yield were increased significantly for each solvent type. However, increment of time did not affect the conversion and bio-oil yield as the temperature affected. 50/50 (v/v) ethanol-acetone mixture gave the highest bio-oil bio oil yield by showing synergistic effects. Highest solid conversion and bio-oil yield were found 64.2% and 44.2 wt.%, respectively. According to GC-MS results, ethyl oleate was the major compound for all solvent ratios that includes ethanol except pure acetone, in which oleic acid was the main component. FT-IR results demonstrated that hemicellulose and cellulose are almost degraded at 300 °C with respect to cellulose and hemicellulose peaks. Parameters effects were also investigated by using statistical analysis. All individual parameters have significant effect on conversion and bio oil yield as well as time-temperature as two-way interactions due to p-values ($p<0.05$). However, time-ratio and temperature-ratio did not show significant effects.

REFERENCES

1. Roman-Leshkov, Y.; Barrett, C. J.; Liu, Z. Y.; Dumesic, J. A., Production of Dimethylfuran for Liquid Fuels from Biomass-derived Carbohydrates. *Nature* **2007**, *447*, 982-986.
2. Kunkes, E. L.; Simonetti, D. A.; West, R. M.; Serrano-Ruiz, J. C.; Gärtner, C. A.; Dumesic, J. A., Catalytic Conversion of Biomass to Monofunctional Hydrocarbons and Targeted Liquid-Fuel Classes. *Science* **2008**, *322*, 417- 421.
3. Bond, J. Q.; Alonso, D. M.; Wang, D.; West, R. M.; Dumesic, J. A., Integrated Catalytic Conversion of γ -Valerolactone to Liquid Alkenes for Transportation Fuels. *Science* **2010**, *327*, 1110-1114.
4. Mazaheri, H.; Lee, K. T.; Mohamed, A. R., Influence of Temperature on Liquid Products Yield of Oil Palm Shell via Subcritical Water Liquefaction in the Presence of Alkali Catalyst. *Fuel Process. Technol.* **2013**, *110*, 197-205.
5. Leng, L.; Li, H.; Yuan, X.; Zhou, W.; Huang, H., Bio-oil Upgrading by Emulsification/microemulsification: A Review. *Energy* **2018**, *161*, 214-232.
6. Pandey, A.; Larroche, C.; Ricke, S. C., *Biofuels: Alternative Feedstocks and Conversion Processes*. Academic Press: San Diego, 2011.
7. Saxena, R. C.; Adhikari, D. K.; Goyal, H. B., Biomass-based Energy Fuel through Biochemical Routes: A review. *Renewable Sustainable Energy Rev.* **2009**, *13*, 167-178.
8. Mazaheri, H.; Lee, K. T.; Bhatia, S.; Mohamed, A. R., Sub/supercritical Liquefaction of Oil Palm Fruit Press Fiber for the Production of Bio-oil: Effect of Solvents. *Bioresour. Technol.* **2010**, *101*, 7641-7647.
9. Karatas, H.; Olgun, H.; Akgun, F., Experimental Results of Gasification of Cotton Stalk and Hazelnut Shell in a Bubbling Fluidized Bed Gasifier under Air and Steam Atmospheres. *Fuel* **2013**, *112*, 494-501.
10. Lu, Y.; Wei , X. Y.; Cao, J.-P.; Peng Li; Liu, F.-J.; Zhao, Y.-P.; Fan, X.; Zhao, W.; Rong, L.-C.; Wei, Y.-B.; Wang, S.-Z.; Zhou, J.; Zong, Z.-M., Characterization of a

Bio-oil from Pyrolysis of Rice Husk by Detailed Compositional Analysis and Structural Investigation of Lignin. *Bioresour. Technol.* **2012**, *116*, 114-119.

11. Madhiyanon, T.; Sathitruangsak, P.; Soponronnarit, S., Influences of Coal Size and Coal-feeding Location in Co-firing with Rice Husks on Performance of a Short-combustion-chamber Fluidized-bed Combustor (SFBC). *Fuel Process. Technol.* **2011**, *92*, 462-470.
12. Gozaydin, G.; Yuksel, A., Valorization of Hazelnut Shell Waste in Hot Compressed Water. *Fuel Process. Technol.* **2017**, *166*, 96-106.
13. Akin, O.; Yuksel, A., Novel Hybrid Process for the Conversion of Microcrystalline Cellulose to Value-added Chemicals: Part 1: Process Optimization. *Cellulose* **2016**, *23*, 3475-3493.
14. Brand, S.; Susanti, R. F.; Kim, S. K.; Lee, H.-s.; Kim, J.; Sang, B.-I., Supercritical Ethanol as an Enhanced Medium for Lignocellulosic Biomass Liquefaction: Influence of Physical Process Parameters. *Energy* **2013**, *59*, 173-182.
15. Huang, H.; Yuan, X.; Zeng, G.; Wang, J.; Li, H.; Zhou, C.; Pei, X.; You, Q.; Chen, L., Thermochemical Liquefaction Characteristics of Microalgae in Sub- and Supercritical Ethanol. *Fuel Process. Technol.* **2011**, *92*, 147-153.
16. Li, H.; Yuan, X.; Zeng, G.; Huang, D.; Huang, H.; Tong, J.; You, Q.; Zhang, J.; Zhou, M., The Formation of Bio-oil from Sludge by Deoxy-liquefaction in Supercritical Ethanol. *Bioresour. Technol.* **2010**, *101*, 2860-2866.
17. Chumpoo, J.; Prasassarakich, P., Bio-Oil from Hydro-Liquefaction of Bagasse in Supercritical Ethanol. *Energy Fuels* **2010**, *24*, 2071-2077.
18. Zhou, D.; Zhang, S.; Fu, H.; Chen, J., Liquefaction of Macroalgae Enteromorpha prolifera in Sub-/Supercritical Alcohols: Direct Production of Ester Compounds. *Energy Fuels* **2012**, *26*, 2342-2351.
19. Jin, B.; Duan, P.; Zhang, C.; Xu, Y.; Zhang, L.; Wang, F., Non-catalytic Liquefaction of Microalgae in Sub-and Supercritical Acetone. *Chem. Eng. J.* **2014**, *254*, 384-392.

20. Akhtar, J.; Amin, N. A. S., A Review on Process Conditions for Optimum Bio-oil Yield in Hydrothermal Liquefaction of Biomass. *Renewable Sustainable Energy Rev.* **2011**, *15*, 1615-1624.

21. Sengupta, D.; Pike, R. W., *Chemicals from Biomass: Integrating Bioprocesses into Chemical Production Complexes for Sustainable Development*. CRC Press: 2013.

22. James H. Clark, F. D., *Introduction to Chemicals from Biomass*. 2nd ed.; Wiley: West Sussex, 2015.

23. Tucker, S. C., Solvent Density Inhomogeneities in Supercritical Fluids. *Chem. Rev.* **1999**, *99*, 391-418.

24. Möller , M.; Nilges , P.; Harnisch, F.; Schröder, U., Subcritical Water as Reaction Environment: Fundamentals of Hydrothermal Biomass Transformation. *ChemSusChem* **2011**, *4*, 566-579.

25. McKendry, P., Energy Production from Biomass (Part 2): Conversion Technologies. *Bioresour. Technol.* **2002**, *83*, 47-54.

26. Chen, H.; Wang, L., *Technologies for Biochemical Conversion of Biomass*. Elsevier: Academic Press, 2017.

27. Fan, S. P.; Zakaria, S.; Chia, C. H.; Jamaluddin, F.; Nabihah, S.; Liew, T. K.; Pua, F. L., Comparative Studies of Products Obtained from Solvolysis Liquefaction of Oil Palm Empty Fruit Bunch Fibres using Different Solvents. *Bioresour. Technol.* **2011**, *102*, 3521-3526.

28. Huang, H.-J.; Yuan, X.-Z.; Zeng, G.-m.; Liu, Y.; Li, H.; Yin, J.; Wang, X.-l., Thermochemical Liquefaction of Rice Husk for Bio-oil Production with Sub- and Supercritical Ethanol as Solvent. *J. Anal. Appl. Pyrolysis* **2013**, *102*, 60-67.

29. Liu, Z.; Zhang, F.-S., Effects of Various Solvents on the Liquefaction of Biomass to Produce Fuels and Chemical Feedstocks. *Energy Convers. Manage.* **2008**, *49*, 3498-3504.

30. Brand, S.; Kim, J., Liquefaction of Major Lignocellulosic Biomass Constituents in Supercritical Ethanol. *Energy* **2015**, *80*, 64-74.

31. Chen, Y.; Wu, Y.; Zhang, P.; Hua, D.; Yang, M.; Li, C.; Chen, Z.; Liu, J., Direct Liquefaction of Dunaliella Tertiolecta for Bio-oil in Sub/supercritical Ethanol-Water. *Bioresour. Technol.* **2012**, *124*, 190-198.

32. Jie Lu, E. C. B., Charles L. Liotta, Charles A. Eckert, Nearcritical and Supercritical Ethanol as a Benign Solvent: Polarity and Hydrogen-bonding. *Fluid Phase Equilib.* **2002**, *198*, 37 - 49.

33. McHugh, M.; Krukonis, V., *Supercritical Fluid Extraction* 2nd ed.; 1994; p 100-105.

34. Isa, K. M.; Abdullah, T. A. T.; Ali, U. F. M., Hydrogen Donor Solvents in Liquefaction of Biomass: A Review. *Renewable Sustainable Energy Rev.* **2018**, *81*, 1259-1268.

35. Zhang, T.; Zhou, Y.; Liu, D.; Petrus, L., Qualitative Analysis of Products Formed during the Acid Catalyzed Liquefaction of Bagasse in Ethylene Glycol. *Bioresour. Technol.* **2007**, *98*, 1454-1459.

36. Hibbert, H.; Rowley, H. J., Studies on Lignin and Related Compounds II. Glycol Lignin and Glycol-ether Lignin. *Can. J. Res.* **1930**, *2*, 364-375.

37. Hibbert, H.; Rowley, H. J., Studies on Lignin and Related Compounds I. A New Method for Isolation of Spruce Wood Lignin. *Can. J. Res.* **1930**, *2*, 357-363.

38. Kobayashi, M.; Asano, T.; Kajiyama, M.; Tomita, B., Analysis on Residue Formation during Wood Liquefaction with Polyhydric Alcohol. *J. Wood Sci.* **2004**, *50*, 407-414.

39. Hu, X.; Wang, Y.; Mourant, D.; Gunawan, R.; Lievens, C.; Chaiwat, W.; Gholizadeh, M.; Wu, L.; Li, X.; Li, C. Z., Polymerization on Heating Up of Bio-oil: A Model Compound Study. *AIChE J.* **2013**, *59*, 888-900.

40. Mortensen, P. M.; Grunwaldt, J. D.; Jensen, P. A.; Knudsen, K. G.; Jensen, A. D., A Review of Catalytic Upgrading of Bio-oil to Engine Fuels. *Appl. Catal., A* **2011**, *407*, 1-19.

41. Wu, L.; Hu, X.; Mourant, D.; Wang, Y.; Kelly, C.; Garcia-Perez, M.; He, M.; Li, C.-Z., Quantification of Strong and Weak Acidities in Bio-oil via Non-aqueous Potentiometric Titration. *Fuel* **2014**, *115*, 652-657

42. A, K.; A, G., Biomass Conversion in Water at 330-410 °C and 30-50 MPa. Identification of Key Compounds for Indicating Different Chemical Reaction Pathways. *Ind. Eng. Chem. Res.* **2003**, *42*, 267-279.

43. Sasaki, M.; Fang, Z.; Fukushima, Y.; Adschari, T.; Arai, K., Dissolution and Hydrolysis of Cellulose in Subcritical and Supercritical Water. *Ind. Eng. Chem. Res.* **2000**, *39*, 2883 - 2890.

44. Saka, S.; Kusdiana, D., Biodiesel Fuel from Rapeseed Oil as Prepared in Supercritical Methanol. *Fuel* **2001**, *80*, 225 - 231.

45. Warabi, Y.; Kusdiana, D.; Saka, S., Reactivity of Triglycerides and Fatty Acids of Rapeseed Oil in Supercritical Alcohols. *Bioresour. Technol.* **2004**, *91*, 283-287.

46. Sawangkeaw, R.; Bunyakiat, K.; Ngamprasertsith, S., A Review of Laboratory-scale Research on Lipid Conversion to Biodiesel with Supercritical Methanol (2001–2009). *J. Supercrit. Fluids* **2010**, *55*, 1-13.

47. Ilharco, L. M.; Brito de Barros, R., Aggregation of Pseudoisocyanine Iodide in Cellulose Acetate Films: Structural Characterization by FTIR. *Langmuir* **2000**, *16*, 9331-9337.

48. Li, M.-F.; Sun, S.-N.; Xu, F.; Sun, R.-C., Formic Acid Based Organosolv Pulping of Bamboo (*Phyllostachys acuta*): Comparative Characterization of the Dissolved Lignins with Milled Wood Lignin. *Chem. Eng. J.* **2012**, *179*, 80-89.

49. Cheng, L.; Ye, X. P.; He, R.; Liu, S., Investigation of Rapid Conversion of Switchgrass in Subcritical Water. *Fuel Process. Technol.* **2009**, *90*, 301-311.

50. Pavlovic, L.; Knez, Y.; Skerget, M., Subcritical Water – a Perspective Reaction Media for Biomass Processing to Chemicals: Study on Cellulose Conversion as a Model for Biomass. *Chem. Biochem. Eng.* **2013**, *27*, 73-82.

APPENDIX A

GC-MS DETECTED COMPOUND LIST

Table A.1. GC-MS results of hazelnut shell liquefaction in ethanol, acetone and their mixtures at 300 °C

No.	RT (min)	Solvent Ratio (EtOH:Ac -v:v%)					Compound
		0:100	25:75	50:50	75:25	100:0	
1	4.167	-	0.45	1.24	1.51	3.78	Butanoic acid, 2-hydroxy-, ethyl ester
2	4.352	0.94	0.43	-	-	-	2-Cyclopenten-1-one, 3,4,5,5-tetramethyl-
3	4.429	-	-	0.50	0.41	0.43	1,3-Dioxolane, 2-(2-propenyl)-
4	4.553	3.28	2.91	3.91	2.03	-	2,5-Hexanedione
5	4.749	0.68	0.54	0.37	-	-	1,3-Dioxolane-4-methanol, 2,2 dimethyl-
6	4.879	1.75	1.02	0.93	0.47	-	3(2H)-Furanone, 2-(1-hydroxy-1-methyl-2-oxopropyl)-2,5-dimethyl-
7	5.105	-	0.53	0.66	0.31	-	2,2-Dimethylbutanedioic acid
8	5.206	2.41	1.14	1.01	0.73	-	2-Cyclopenten-1-one, 3-methyl-
9	5.461	-	-	0.65	0.42	0.56	Methanone, dicyclopropyl-
10	5.520	-	0.89	1.46	0.99	-	Cyclohexane, 1-methyl-4-methylene-
11	5.639	1.11	1.45	2.04	1.40	-	L-borneol
12	5.750	-	-	-	0.47	1.07	1-Hepten-4-ol
13	5.864	1.23	-	-	-	-	trans-2-Methyl-4-hexen-3-ol
14	5.929	-	0.69	0.61	0.51	-	1H-Pyrrole, 2-ethyl-4-methyl-
15	6.16	2.22	1.85	2.35	0.11	-	3,6-Heptanedione
16	6.374	3.05	2.24	3.00	1.86	-	Butanoic acid, 4-hydroxy-2-methylene-
17	6.469	-	0.79	1.00	0.38	-	1,2,4,4-Tetramethylcyclopentene
18	6.516	1.01	-	-	-	-	2,2-Dimethylocta-3,4-dienal
19	6.600	-	0.63	0.57	0.42	-	1H-Pyrrole, 3-ethyl-2,4-dimethyl-
20	6.660	0.52	0.77	0.75	0.52	0.79	2-Cyclohexen-1-one, 3-methyl-
21	6.729	-	0.74	1.07	0.80	0.86	Pentanoic acid, 4-oxo-, ethyl ester

(Cont on the next page)

Table A.1 (Cont)

No.	RT (min)	Solvent Ratio (EtOH:Ac -v:v%)					Compound
		0:100	25:75	50:50	75:25	100:0	
22	6.907	0.94	0.66	0.81	0.48	-	Nona-3,5-dien-2-one
23	6.984	2.32	3.94	5.23	4.03	6.02	Propanoic acid, 2-methyl-, anhydride
24	7.076	0.81	0.45	-	-	-	Phenol, 3-methyl-
25	7.168	4.01	3.11	0.44	3.23	4.74	Phenol, 2-methoxy-
26	7.316	1.48	-	-	-	-	3,3-Dimethyl-hepta-4,5-dien-2-one
27	7.364	1.28	4.41	4.28	2.91	-	2-Cyclohexen-1-one, 3,5-dimethyl-
28	7.447	2.56	0.94	-	-	-	2,5-Heptadien-4-one, 2,6-dimethyl-
29	7.619	1.35	0.72	0.72	0.36	0.81	2-Cyclopenten-1-one, 3-ethyl-2-hydroxy-
30	7.94	0.44	-	-	-	-	E-6-Octadecen-1-ol acetate
31	7.986	-	-	0.18	0.49	0.96	Cyclohexylideneacetic acid
32	8.354	0.90	-	-	-	-	Cyclohexanone, 2-acetyl-
33	8.392	-	1.10	0.34	1.48	1.96	Butanedioic acid, diethyl ester
34	8.49	1.02	1.19	1.71	0.58	-	2-Acetonylcyclopentanone
35	8.6	1.54	1.15	0.57	1.19	1.56	Phenol, 2-methoxy-4-methyl-1,4-Benzenediol, 2,5-dimethyl-
36	8.668	1.46	1.09	0.71	0.28	-	Butanedioic acid, 2-isopropenyl-2-methyl-
37	9.125	-	-	1.49	1.49	2.27	1,3-Dioxolane, 4-ethyl-4-methyl-2-pentadecyl-
38	9.303	-	-	-	0.47	0.39	2-Cyclohexen-1-one, 4-(1-methylethyl)-
39	9.308	1.58	1.15	1.08	0.38	-	Tetradecanoic acid, 2-hydroxy-
40	9.522	-	-	0.59	1.75	0.63	Pentanedioic acid, diethyl ester
41	9.652	-	-	0.83	0.96	1.12	Phenol, 4-ethyl-2-methoxy-2-Cyclohexen-1-one, 2-hydroxy-3-methyl-6-(1-methylethyl)-
42	9.694	5.81	3.73	4.57	3.98	3.74	7-Methyl-Z-tetradecen-1-ol acetate
43	9.777	-	0.63	0.64	0.38	-	4-(1,5-Dihydroxy-2,6,6-trimethylcyclohex-2-enyl)but-3-en-2-one
44	10.120	-	0.48	0.89	0.60	-	Cyclohexanone, 2-(hydroxymethylene)-3-methyl-6-(1-methylethyl)-
45	10.252	-	0.61	0.51	0.52	-	Phenol, 2,6-dimethoxy-
46	10.328	2.67	1.20	0.72	0.32	-	Phenol, 2-methoxy-5-(1-propenyl)-(E)-
47	10.553	1.72	1.77	0.96	2.10	2.76	(Cont on the next page)
48	10.621	1.36	0.69	2.22	0.71	-	56

Table A.1 (Cont)

No.	RT (min)	Solvent Ratio (EtOH:Ac -v:v%)					Compound
		0:100	25:75	50:50	75:25	100:0	
49	10.725	2.91	1.64	0.54	1.81	2.57	Phenol, 2-methoxy-4-propyl-
50	10.986	-	-	2.17	1.79	2.25	Ethyl beta-D-riboside
51	11.188	2.98	0.84	0.98	0.83	-	2,5-Cyclohexadiene-1,4-dione, 2-methyl-5-(1-methylethyl)-
52	11.291	-	0.39	0.93	1.42	1.39	D-Galactose, 6-deoxy-
53	11.360	1.14	0.40	0.37	-	-	1,4-Methanoazulen-7-ol, decahydro-1,5,5,8a-tetramethyl-, [1s-(1 α ,3 α ,4 α ,7 β ,8a β)]-[1,1'-Bicyclopentyl]-2-octanoic acid, 2'-hexyl-, methyl ester
54	11.591	0.14	0.40	0.42	0.38	1.64	Phenol, 2-methoxy-4-(1-propenyl)-, (E)-
55	11.644	-	1.90	0.95	1.33	1.15	Cyclopropane[<i>c,d</i>]pentalene-1,3-dione, hexahydro-4-(2-methyl-2-propenyl)-2,2,4-trimethyl-
56	11.804	-	1.48	1.21	1.10	-	2(3H)-Naphthalenone, 4,4a,5,6,7,8-hexahydro-1-methoxy-
57	12.059	1.89	1.23	1.76	-	-	5-Hepten-3-yn-2-ol, 6-methyl-5-(1-methylethyl)-
58	12.071	-	-	1.04	0.75	0.48	5-tert-Butylpyrogallol
59	12.433	0.87	1.30	0.87	0.81	0.52	2-Propanone, 1-(4-hydroxy-3-methoxyphenyl)-
60	12.522	1.71	1.63	0.80	1.07	0.98	4H-1-Benzopyran-4-one, 2,3-dihydro-7-hydroxy-2,2-dimethyl-
61	12.723	1.55	-	-	-	-	Benzoic acid, 4-hydroxy-3-methoxy-, ethyl ester
62	13.055	-	0.97	0.82	0.81	0.66	Benzene, 1,1'-tetradecylidenebis-
63	13.266	1.16	0.62	0.50	0.56	1.05	Phenylacetylformic acid, 4-hydroxy-3-methoxy-
64	13.601	-	-	0.41	1.06	0.55	2-Butanone, 4-(4-hydroxy-3-methoxyphenyl)-
65	13.677	1.09	1.70	0.33	1.12	1.00	1H-Indene, 3-butyl-1-methyl-
66	14.194	2.20	-	-	-	-	2-[4-methyl-6-(2,6,6-trimethylcyclohex-1-enyl)hexa-1,3,5-trienyl]cyclohex-1-en-1-carboxaldehyde
67	14.733	1.21	0.71	-	-	-	Pentadecanoic acid, 14-methyl-, methyl ester
68	16.601	1.05	0.52	-	-	-	(Cont on the next page)

Table A.1 (Cont)

No.	RT (min)	Solvent Ratio (EtOH:Ac -v:v%)					Compound
		0:100	25:75	50:50	75:25	100:0	
69	17.057	2.87	0.78	0.76	-	-	n-Hexadecanoic acid
70	17.399	-	2.42	0.18	3.22	4.51	Hexadecanoic acid, ethyl ester
71	18.568	0.52	0.52	0.36	0.59	0.5	Linoleic acid ethyl ester
74	19.335	-	3.68	2.93	4.92	6.76	9,12-Octadecadienoic acid, ethyl ester
75	19.429	-	18.25	22.90	27.79	34.63	Ethyl Oleate
76	19.665	-	1.48	1.34	1.66	1.87	Octadecanoic acid, ethyl ester 3-(3-Hydroxy-4-methoxyphenyl)-l-alanine4-Hydroxy-4-(1-methoxycyclopropyl)-3,3,5,8,10,10-hexamethyltricyclo[6.2.2.0(2,7)]dodeca-5,11-dien-9-one
77	21.273	2.01	1.08	0.77	1.07	1.15	
78	30.169	1.98	1.69	0.73	1.32	0.95	β-Sitosterol

APPENDIX B

GC-MS CHROMATOGRAMS

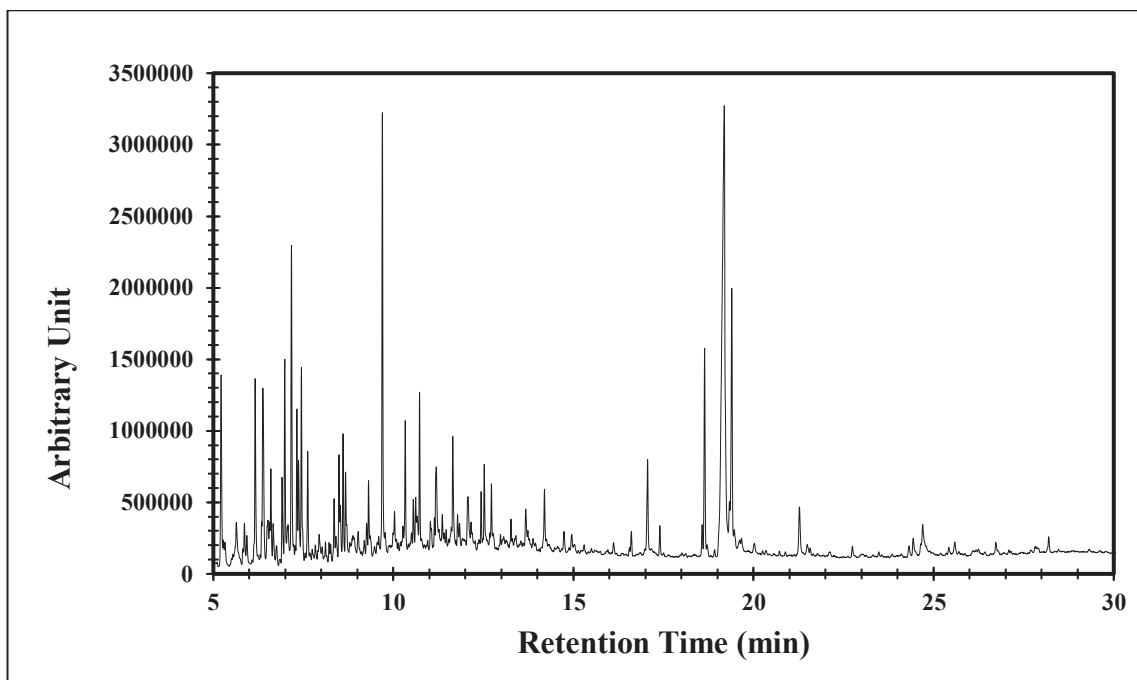


Figure B.1. GC-MS Chromatogram of 300 °C, 90 min, 0:100 ethanol/acetone (v/v%)

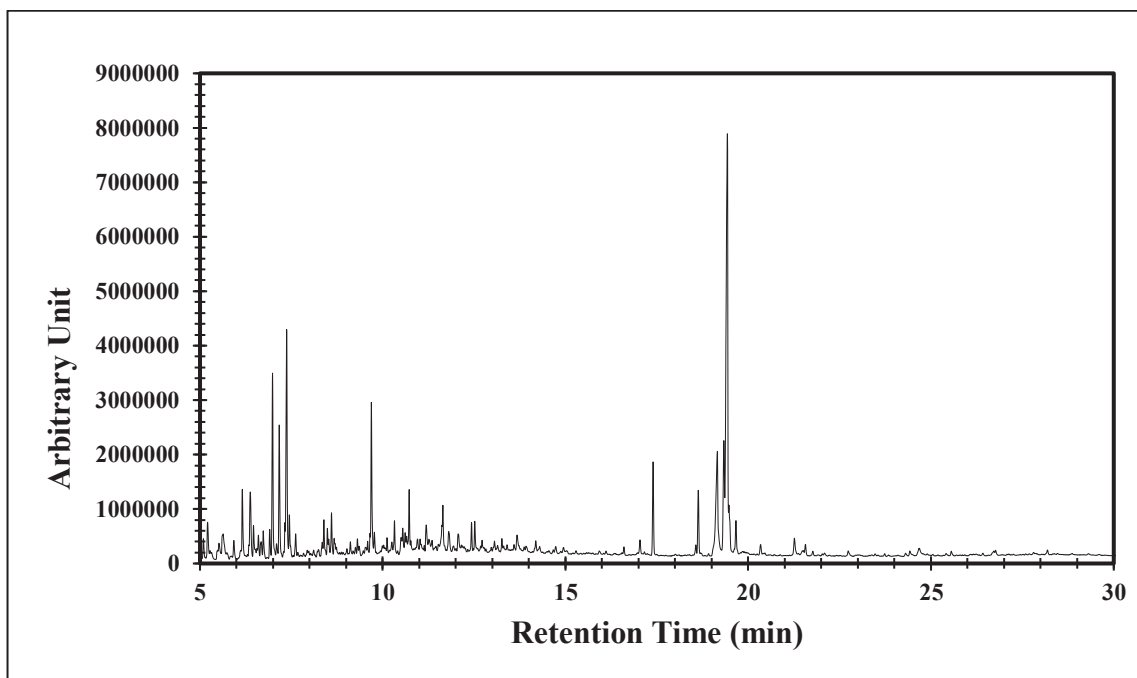


Figure B.2. GC-MS Chromatogram of 300 °C, 90 min, 25:75 ethanol/acetone (v/v%)

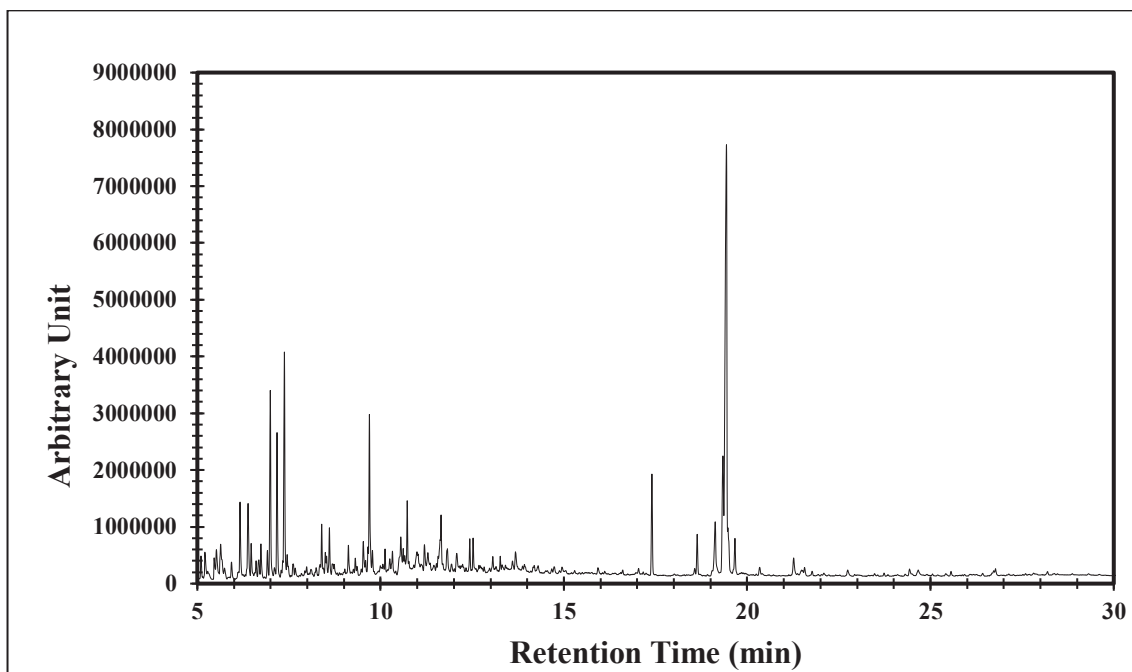


Figure B.3. GC-MS Chromatogram of 300 °C, 90 min, 50:50 ethanol/acetone (v/v%)

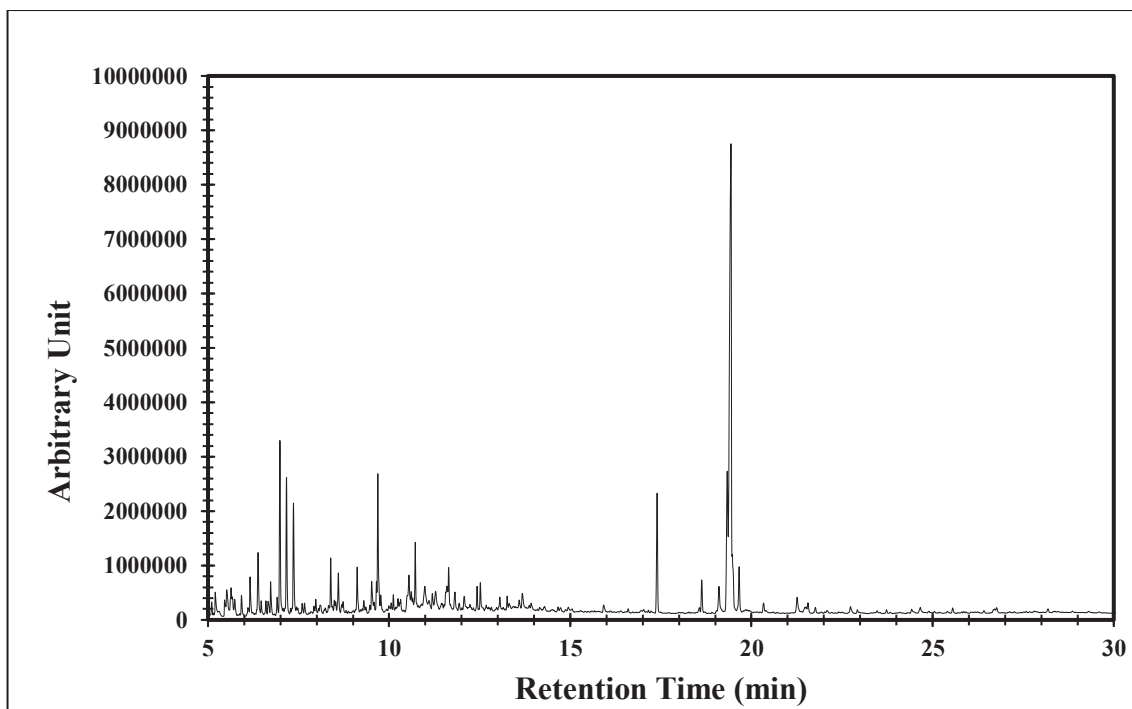


Figure B.4. GC-MS Chromatogram of 300 °C, 90 min, 75:25 ethanol/acetone (v/v%)

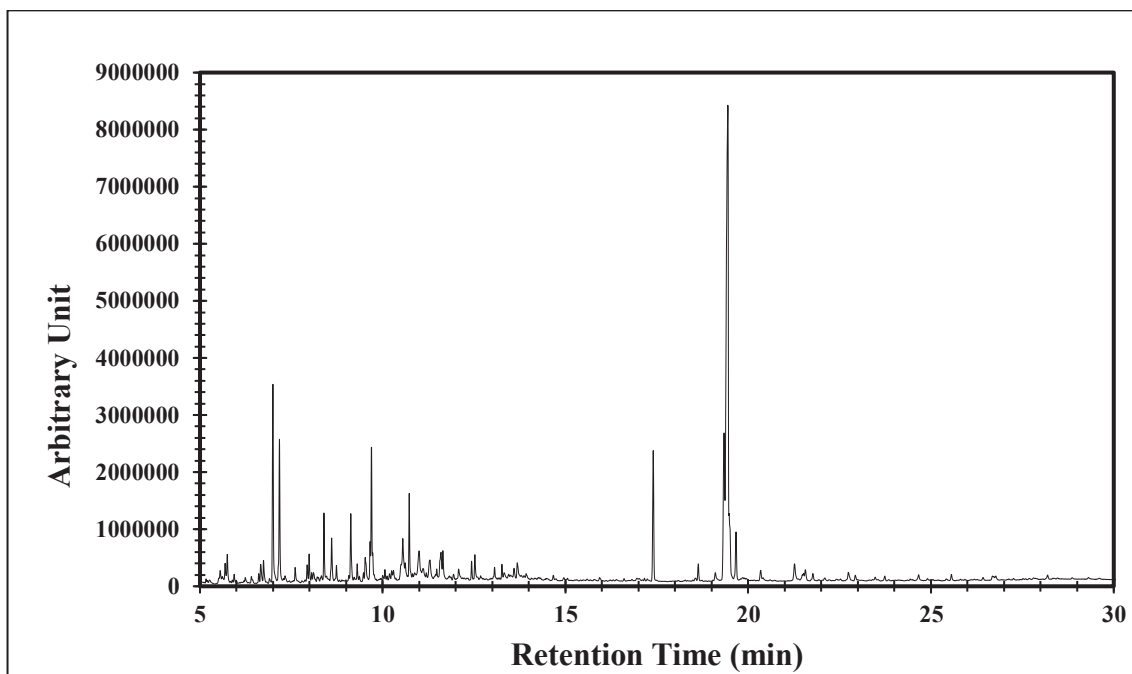


Figure B.5. GC-MS Chromatogram of 300 °C, 90 min, 100:0 ethanol/acetone (v/v%)

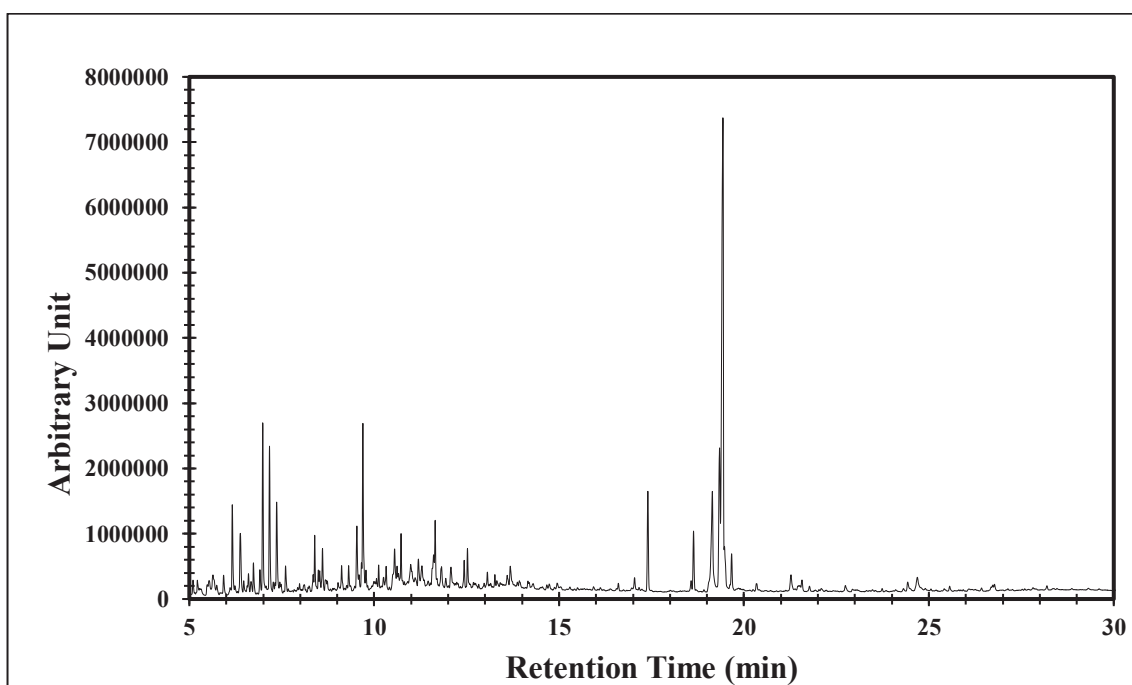


Figure B.6. GC-MS Chromatogram of 300 °C, 60 min, 50:50 ethanol/acetone (v/v%)

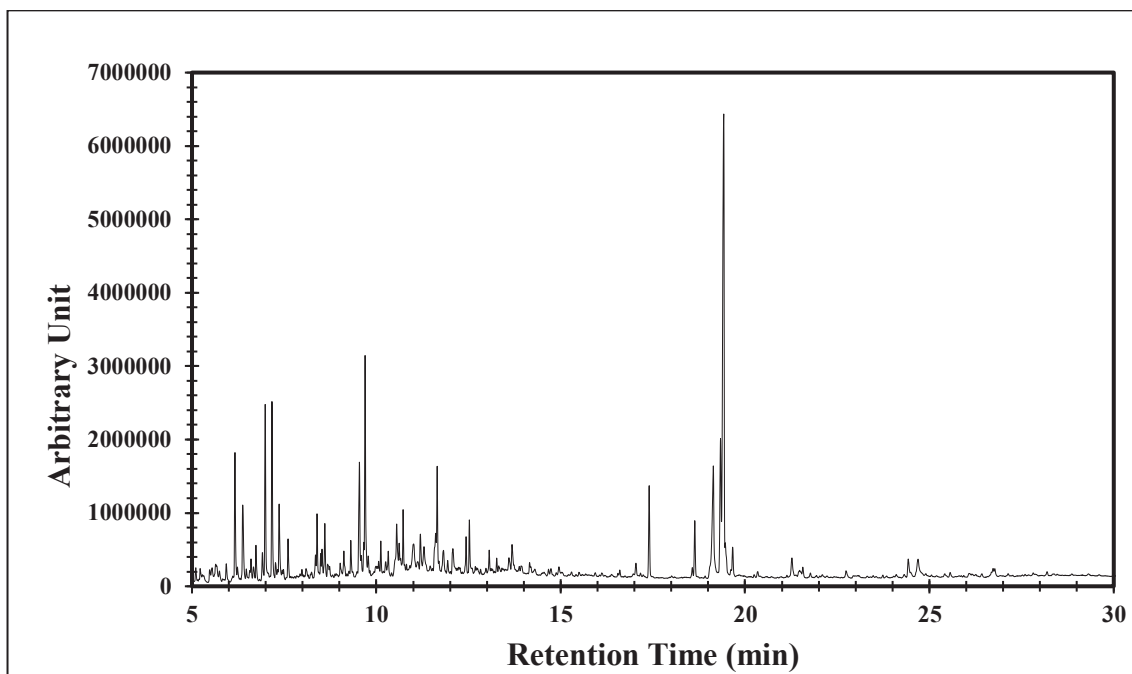


Figure B.7. GC-MS Chromatogram of 300 °C, 30 min, 50:50 ethanol/acetone (v/v%)

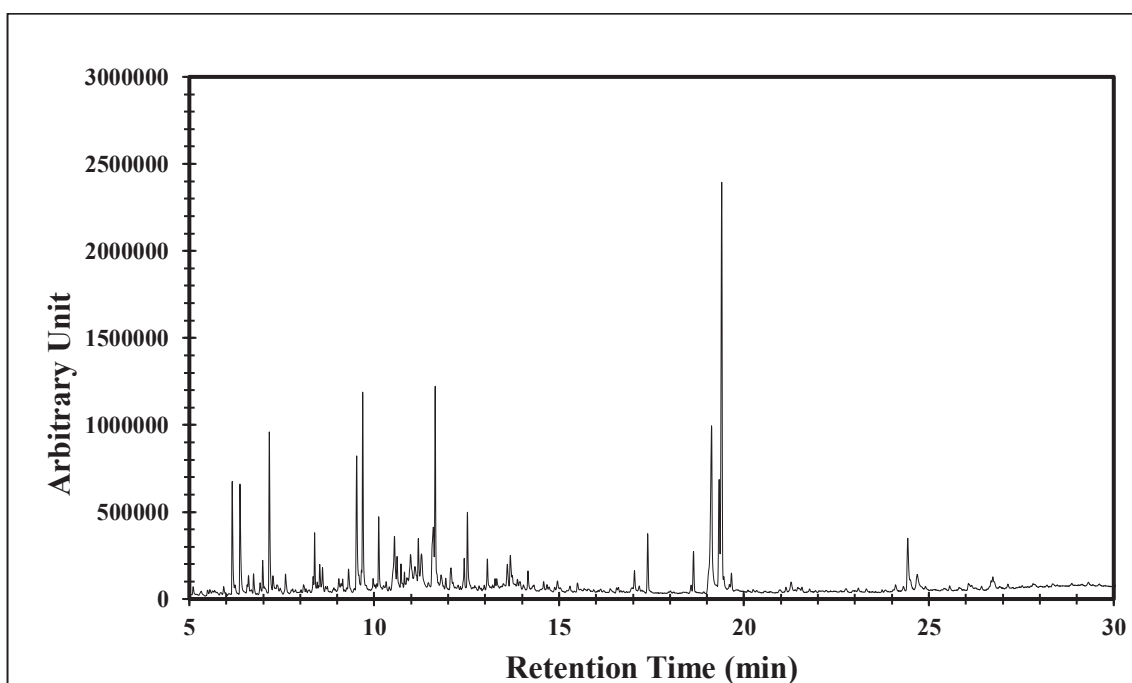


Figure B.8. GC-MS Chromatogram of 260 °C, 90 min, 50:50 ethanol/acetone (v/v%)

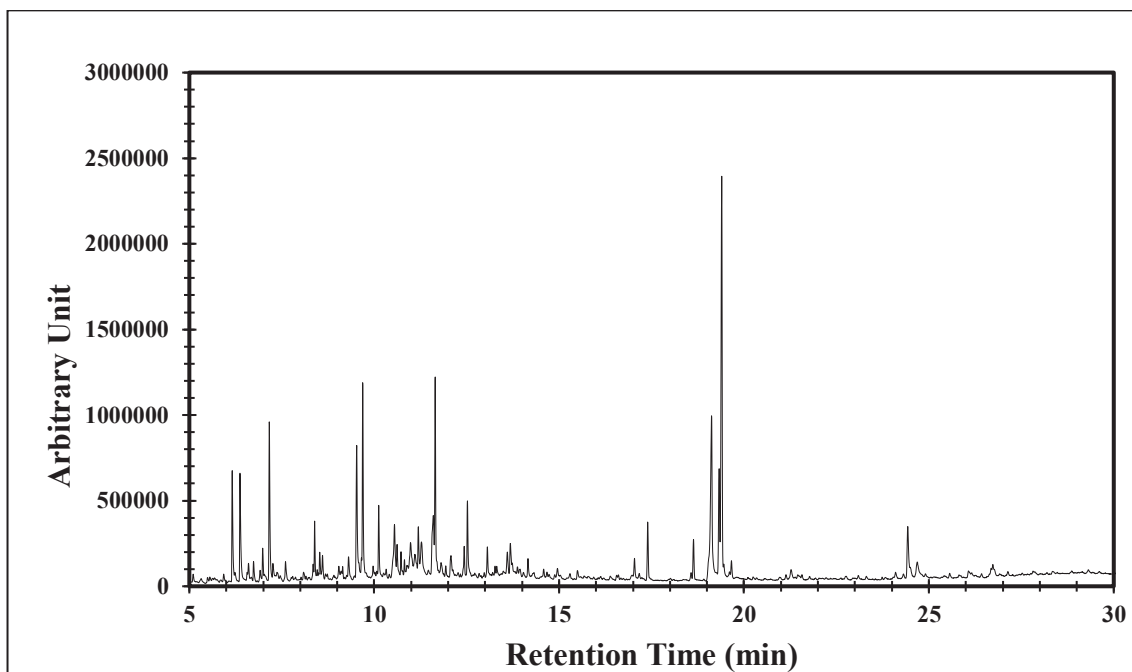


Figure B.9. GC-MS Chromatogram of 260 °C, 60 min, 50:50 ethanol/acetone (v/v%)

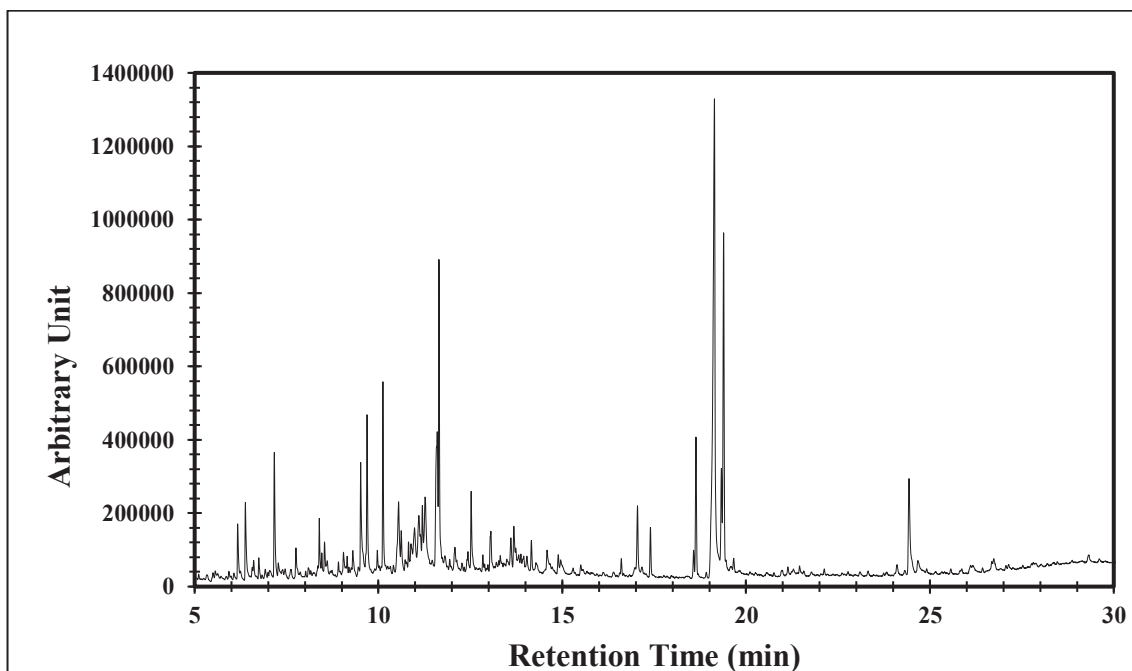


Figure B.10. GC-MS Chromatogram of 260 °C, 30 min, 50:50 ethanol/acetone (v/v%)